Mechanisms of Selective Monocyte Targeting by Liposomes Functionalized with a Cationic, Arginine-Rich Lipopeptide

Münter, Rasmus; Bak, Martin; Christensen, Esben; Kempen, Paul; Larsen, Jannik; Kristensen, Kasper; Parhamifar, Ladan; Andresen, Thomas Lars

Published in:
Acta Biomaterialia

Link to article, DOI:
10.1016/j.actbio.2022.03.029

Publication date:
2022

Document Version
Peer reviewed version

Journal Pre-proof

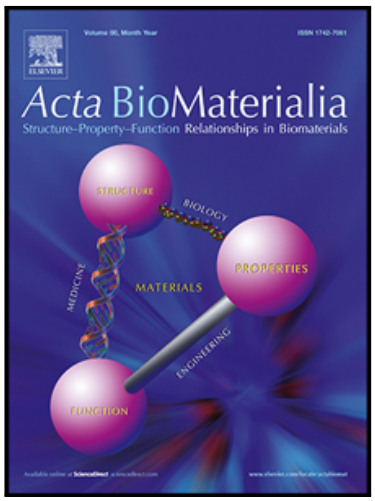

Mechanisms of Selective Monocyte Targeting by Liposomes Functionalized with a Cationic, Arginine-Rich Lipopeptide

Rasmus Münter , Martin Bak , Esben Christensen , Paul Kempen , Jannik Larsen , Kasper Kristensen , Ladan Parhamifar , Thomas Lars Andresen

PII: S1742-7061(22)00159-3
DOI: https://doi.org/10.1016/j.actbio.2022.03.029
Reference: ACTBIO 7928

To appear in: *Acta Biomaterialia*

Received date: 4 October 2021
Revised date: 8 March 2022
Accepted date: 13 March 2022

Please cite this article as: Rasmus Münter , Martin Bak , Esben Christensen , Paul Kempen , Jannik Larsen , Kasper Kristensen , Ladan Parhamifar , Thomas Lars Andresen , Mechanisms of Selective Monocyte Targeting by Liposomes Functionalized with a Cationic, Arginine-Rich Lipopeptide, *Acta Biomaterialia* (2022), doi: https://doi.org/10.1016/j.actbio.2022.03.029

Mechanisms of Selective Monocyte Targeting by Liposomes Functionalized with a Cationic, Arginine-Rich Lipopeptide

Rasmus Münter[a], *Martin Bak*[a], *Esben Christensen*[a], *Paul Kempen*[a,b], *Jannik Larsen*[a], *Kasper Kristensen*[a], *Ladan Parhamifar*[a], *Thomas Lars Andresen*[a,*]

[a] Biotherapeutic Engineering and Drug Targeting, Department of Health Technology, Technical University of Denmark, 2800 Kgs. Lyngby, Denmark

[b] DTU Nanolab, The National Centre for Nano Fabrication and Characterization, Technical University of Denmark, 2800 Kgs. Lyngby, Denmark

*Corresponding author. Email: tlan@dtu.dk. Telephone: +45 25374486

Graphical Abstract

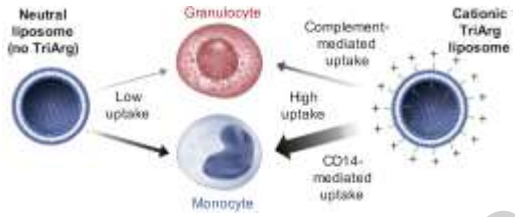

Keywords: Cationic liposome, immunotherapy, CD14, complement, monocyte

Abstract:

Stimulation of monocytes with immunomodulating agents can harness the immune system to treat a long range of diseases, including cancers, infections and autoimmune diseases. To this end we aimed to develop a monocyte-targeting delivery platform based on cationic liposomes, which can be utilized to deliver immunomodulators and thus induce monocyte-mediated immune responses while avoiding off-target side-effects. The cationic liposome design is based on functionalizing the liposomal membrane with a cholesterol-anchored tri-arginine peptide (TriArg). We demonstrate that TriArg liposomes can target monocytes with high specificity in both human and murine blood and that this targeting is dependent on the content of TriArg in the liposomal membrane. In addition, we show that the mechanism of selective monocyte targeting involves the CD14 co-receptor, and selectivity is

compromised when the TriArg content is increased, resulting in complement-mediated off-target uptake in granulocytes. The presented mechanistic findings of uptake by peripheral blood leukocytes may guide the design of future drug delivery systems utilized for immunotherapy.

1. Introduction

Immunotherapy is increasingly accepted as an appealing and effective alternative to conventional treatment options [1], potentially allowing effective treatment of a variety of diseases, including cancers, infections, and autoimmune diseases [2–4] . Vaccines against both cancers and infectious diseases typically rely on delivery of an adjuvant and an antigen to dendritic cells (DCs) [5–7]. An attractive, alternative approach to orchestrating a desired DC response is to target circulating monocytes, which are readily accessible in the blood upon intravenous administration [8,9]. Monocytes can differentiate into DCs upon specific activation, present delivered antigen [9], and can activate both the innate and adaptive immune system. Unspecific activation, such as activation of TLRs in off-target cell populations, can potentially lead to pro-tumorigenic inflammation [10] or side effects such as allergic reactions and septic shock [11], underscoring the advantage of a targeting delivery platform.

Liposomal formulations can serve as excellent immune cell-targeting drug delivery platforms of adjuvants and antigens [12–15]: Liposomes demonstrate low toxicity and offer the possibility to carry both hydrophilic and hydrophobic drugs [12–15]. Additionally, they are versatile with respect to engineering their surface structure and are relatively easy to manufacture [16–18]. The biocompatible nature of liposomes renders them optimal for specific targeting of preferred immune cell subsets and controlling the type and extent of immune response evoked by the adjuvants and antigens they carry [19,20]. Our group has previously demonstrated a delivery platform targeting monocytes using cationic DOTAP-based liposomes [21], showing that the targeted monocytes differentiated into monocyte-derived DCs when the liposomes were loaded with a TLR7 agonist. The targeting capability of the liposomes was based on a specific range of cationic charge: Whereas neutral liposomes did not associate to leukocytes and highly cationic liposomes associated equally to all types of leukocytes,

liposomes with an intermediate cationic charge induced specific liposome uptake by monocytes. This simplicity in design is advantageous compared to antibody-based targeting in relation to clinical translation [21]. Thus, cationic liposomes may represent a highly promising platform for targeting and activating monocytes specifically in the blood.

Previous studies have shown that cationic peptides, in particular arginine-rich peptides, offer a unique ability to cross cellular membranes with various cargoes [22–24]. Conjugation of an arginine-rich peptide to a cholesterol anchor creates an amphiphilic construct that can be inserted into liposomal membranes and facilitate cellular internalization of the liposomes [25]. Although a subject of some debate, it is generally believed that arginine-rich peptides conjugated to large cargoes enter cells through endocytosis [24,26–28], thus allowing for activation of TLR-7, -8 and -9 receptors in the endosomes for monocyte stimulation [29]. Consequently, liposomes functionalized with arginine-rich peptides could potentially target monocytes through their cationic charge and at the same time induce effective internalization.

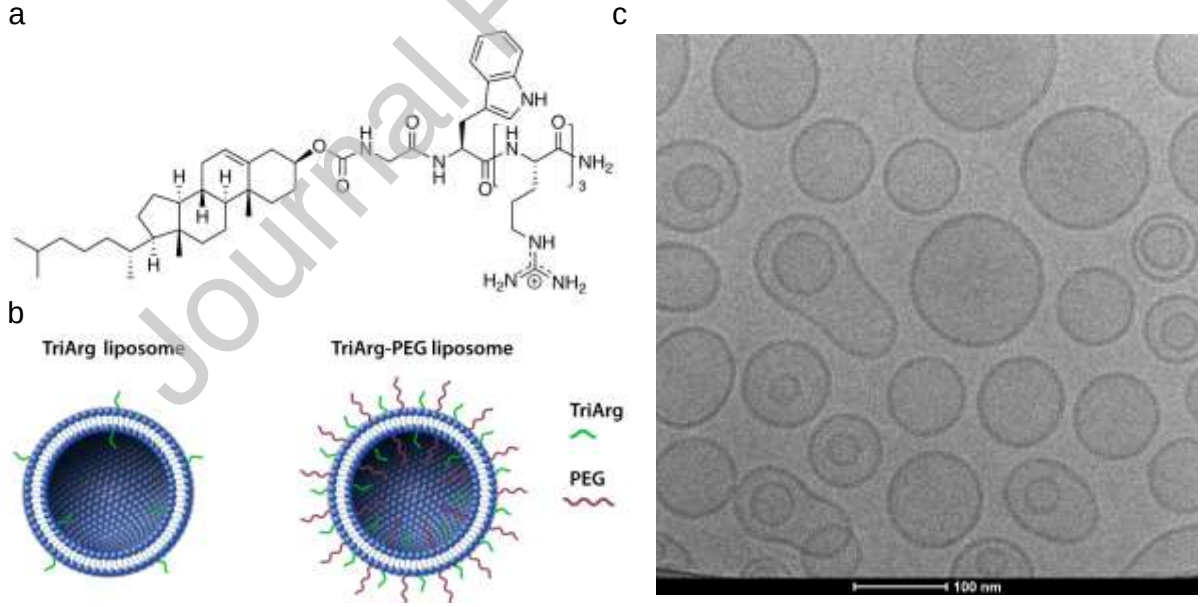

Fig. 1. Liposomes functionalized with the TriArg lipopeptide

Liposome formulations used in the study. (a) The structure of the TriArg compound (Cholesterol-GWRRR). (b) TriArg liposomes were formulated both with and without DOPE-PEG$_{2000}$. (c) Cryogenic transmission electron microscopy (cryoTEM) image of PEGylated liposomes with 6% TriArg lipopeptide.

In the present work, we synthesized a cationic lipopeptide consisting of three arginine residues (TriArg) conjugated to a cholesterol anchor (Fig. 1), facilitating incorporation into a series of liposome formulations with and without polyethylene glycol (PEG). A Trp residue was also included in the lipopeptide, as earlier studies have shown that the presence of tryptophans in polyarginines improves their ability to enter cells [30–33]. The aim was to investigate whether liposomal monocyte targeting could be achieved with these peptide-based cationic constructs and to investigate the mechanisms behind the monocyte targeting in whole human blood (WHB).

We demonstrate that cationic TriArg liposomes, depending on design, can selectively target monocytes in both human blood *ex vivo* and murine blood *in vivo*. The leukocyte uptake pattern, and hence the monocyte targeting capabilities, were dependent on the TriArg content and hence surface charge, which correlate with our previous findings for cationic DOTAP liposomes [21]. We find that the monocyte targeting is mediated by CD14 co-receptor binding, which is abundantly expressed by monocytes. We furthermore show that the complement system, which is known to be implicated in liposomal clearance by leukocytes [34–36], direct off-target uptake in granulocytes depending on the liposome surface charge. These mechanistic findings may help guide the design of new, improved monocyte-targeted liposome formulations.

2. Materials and methods:

2.1. Materials

All chemicals were purchased from Sigma-Aldrich Inc. (Broendby, Denmark) unless otherwise stated. *O*-(7-Azabenzotriazol-1-yl)-*N,N,N′,N′*-tetramethyluronium hexafluorophosphate (HATU) and all Fmoc protected amino acids used for the solid phase peptide synthesis were purchased from Iris-Biotech (Marktredwitz, Germany). Tentagel® Rink Amide Resin used for the solid phase peptide synthesis was purchased from GL Biochem (Shanghai, China). 1-palmitoyl-2-oleoyl-*sn*-glycero-3-phosphocholine (POPC) was purchased from Lipoid GmbH (Ludwigshafen, Germany). Cholesterol, 1-palmitoyl-2-(dipyrrometheneboron difluoride)-undecanoyl-*sn*-glycero-3-phosphocholine (TopFluor PC), and 1,2-dioleoyl-*sn*-glycero-3-phosphoethanolamine-N-[methoxy(polyethylene glycol)-2000](NH_4^+ salt) (DOPE-PEG_{2000}) were purchased from Avanti Polar Lipids (Alabaster, AL, US). Buffers for liposomes, DLS and zeta potential measurements were prepared using chemicals purchased from Merck (Darmstadt, Germany). For washing cells, fetal bovine serum (FBS) was purchased from Biowest (Nuaillé, France). Primary APC-labelled CD14 antibodies for staining in flow cytometry were purchased from BD Biosciences (Becton Dickinson, Franklin Lakes, NJ, US). Anti-CD14 (clone 18D11) for blocking studies and control antibody (MOPC-21) was purchased from Hycult Biotech (Uden, The Netherlands). The LDH toxicity assay (CytoTox 96) was purchased from Promega (Madison, WI, US). All chemicals and reagents were of analytical grade and used without further purification.

2.2. Synthesis instrumentation

Analytical reversed-phase high-performance liquid chromatography (RP-HPLC) was performed on a Gilson HPLC (Gilson Valvemate, UV/Vis-155, 321 Pump, 234 Auto injector) by employing a Waters XTerra C18 or XBridge C18 (5 μm, 4.6 x 150 mm) column. Semi-preparative HPLC was performed on a Waters Semi-preparative HPLC equipped with a Waters 600 Pump & Controller and a Waters 2489 UV/Vis Detector using a Waters XTerra C18 (5 μm, 19 x 150 mm) or a Knauer Eurosphere 100-5 C18 (20 x 250 mm) column. HPLC Eluent A consisted of a 5% CH_3CN aqueous solution with 0.1% trifluoroacetic acid (TFA); HPLC Eluent B consisted of 0.1% TFA in CH_3CN. Preparative HPLC analysis was monitored using UV/Vis detection at 220/280 nm. Mass spectra were recorded on a

Bruker Autoflex™ MALDI-TOF MS Spectrometer using 2,5-dihydroxybenzoic acid (DHB) spiked with sodium trifluoroacetate in CH_3OH as matrix. The Trp residue included in the TriArg peptide allowed for determination of the concentration by measuring absorbance at 280 nm using a Nanodrop 2000c spectrophotometer (Thermo Fisher Scientific, Waltham, MA, US).

2.3. Synthesis of Chol-GWR_3

The peptide H-GWR_3-NH_2 was synthesized by standard solid phase peptide synthesis (SPPS) on a Tentagel Rink Amide resin (Scale: 0.5 mmol; loading: 0.20 mmol g^{-1}) by standard Fmoc methodology. Each coupling was performed using 4.0 equiv Fmoc protected amino acid, 3.95 equiv HATU, and 8 equiv 2,4,6-collidine in DMF for 30 min at room temperature (RT). Deprotection of the Fmoc-protection group was achieved by subjecting the resin to 2x5 min of 20% piperidine in DMF. The first glycine residue was double-coupled first with 5 min 75 °C in a microwave and subsequently 30 min at RT. The resin was cleaved with TFA:TIPS:H_2O (95:2.5:2.5) for 3 h. The solvent was removed in vacuo and the crude peptide was precipitated in cold diethyl ether. The isolated white peptide powder was purified by semi-preparative HPLC by employing a Knauer Eurosphere 100-5 C18 (20 x 250 mm) column. Gradient profile: Linear gradient from 0% B to 20% B over 20 min. R_f-value = 10 min. Flow rate: 17 mL min^{-1}. UV detection at 220/280 nm. The solvent was removed in vacuo and the product lyophilized from a mixture of H_2O and CH_3CN to give a white fluffy powder (0.203 mmol, 41%, purity 90-95%). MALDI-TOF MS (*m/z*): Calc. mass $[M + H]^+$: 729.86, found mass $[M + H]^+$: 729.81. A flamedried RB flask was fitted with a magnet, septum and N_2-atmosphere. The lyophilized peptide (0.101 mmol) was dissolved in dry DMF (75 mL) and added to the RB flask followed by adding DIPEA (441 µL, 2.533 mmol). Cholesteryl chloroformate (55 mg, 0.122 mmol) was dissolved in CH_2Cl_2 (25 mL) and added to the RB flask. The reaction was left to react overnight. The solvent was removed in vacuo and the crude cholesteryl-GWR_3-NH_2 was purified by semi-preparative HPLC by employing a Knauer Eurosphere 100-5 C18 (20 x 250 mm) column. Gradient profile: Linear gradient from 50% B to 100% B over 20 min. R_f-value = 12 min. Flow rate: 17 mL min^{-1}. UV detection at 220/280 nm. The solvent was removed in vacuo and the product lyophilized from a mixture of H_2O and CH_3CN to give a white fluffy powder (0.085 mmol, 84%, purity >98%). Purity assessment was

done by analytical HPLC, see Supplementary Fig. S1). MALDI-TOF MS (*m*/*z*): Calc. mass $[M+H]^+$ = 1142.51; found mass $[M+H]^+$ = 1142.19 (spectrum shown in Supplementary Fig. S2). The overall yield was 34%. The charge properties of the TriArg lipopeptide across various pH values are shown in Supplementary Fig. S3, the logD profile is shown in Supplementary Fig. S4. These physicochemical properties of the TriArg lipopeptide was calculated using the Chemicalize software (ChemAxon, Budapest, Hungary).

2.4. Synthesis of Compstatin analog (4W9A)

The 4W9A Compstatin peptide analog, Ac-ICVWQDWGAHRCT-NH_2, was synthesized by SPPS on a Tentagel Rink Amide resin (Scale: 0.092 mmol; loading: 0.20 mmol/g) by standard Fmoc methodology. Each coupling was performed using 4.0 equiv Fmoc protected amino acid, 3.95 equiv HATU, and 8 equiv 2,4,6-collidine in DMF for 5 min with 75 °C in a microwave. The arginine residue was coupled at RT for 30 min. Deprotection of the Fmoc-protection group was achieved by subjecting the resin to 2x5 min of 20% piperidine in DMF. The initial threonine residue was double-coupled first with 5 min 75 °C in a microwave and subsequently 30 min at RT. Acetic anhydride in DMF (4 M) was used for capping after the final isoleucine and first threonine residue. The resin was cleaved with TFA:TIPS:H_2O:EDT (20 mL, 94:1:2.5:2.5) for 2.5 h. The resin was washed with cleavage mix once and 5 times with CH_2Cl_2. The solvent was removed in vacuo and the crude peptide was precipitated in cold diethyl ether. The crude compound was dissolved in 30% CH_3CN in water with 0.1% TFA (148 mL) and the pH was adjusted to 7-8 using 0.1 M NaOH. Diluted H_2O_2 (1:100, 6 mL) was added to the solution under vigorous stirring. The cyclization was monitored by MALDI-TOF MS and HPLC. Full conversion was observed after 2 h. The resulting solution was lyophilized. The isolated white peptide powder was purified by semi-preparative HPLC by using Waters Xterra prep. RP C18 (5 µm, 19 x 150 mm) column. Gradient profile: Linear gradient from 0% B to 40% B over 30 min. R_f-value = 18 min. Flow rate: 17 mL min^{-1}. UV detection at 220/280 nm. The clean fractions were pooled, lyophilized and resulting in white fluffy powder. The pure compound was re-dissolved and loaded onto a SPE cartridge (Strata® C8, 55 µm, 70 Å, 2 g, 12 mL) for salt swapping. The cartridge was prepared (20 mL of 100%, 50% and 5% CH_3CN in water) followed by loading the compound in <10% CH_3CN in

water (10 mL). The column was flushed with water (100 mL), water with 1% acetic acid (100 mL) and the compound was eluted with 2x50 mL of 50%, 60% and 70% CH_3CN in water with 0.1% acetic acid. The desired fractions were lyophilized again giving a white fluffy powder (0.015 mmol, 16% yield, purity >97%). MALDI-TOF MS (*m/z*): Calc. mass $[M+H]^+$: 1613.70; found mass $[M+H]^+$: 1613.73.

2.5. Liposome formulation

Lipids in powder forms were dissolved in *tert*-butanol:MQ water 9:1, mixed into the desired molar ratios, and freeze-dried overnight. The lipid films were generally hydrated in a sterile 10 mM phosphate buffer (pH 7.0) with 150 mM NaCl to a concentration of 20-25 mM total lipid, and put under magnet stirring for minimum 1 h at 40 °C with vortexing every 20 min. Size of the liposomes were controlled by extruding 21 times through a 100 nm Whatman filter using an Avanti mini-extruder on a heating block at 40 °C.

To prepare gadolinium (Gd)-loaded liposomes for *in vivo* experiments, the lipid films were rehydrated in a buffer containing 10 mM HEPES, 137.5 mM NaCl and 10 mM DOTA(Gd), pH 7.4. After 1 h under 45 °C heating and magnetic stirring, the samples were exposed to 11 freeze-thaw cycles, by repeatedly placing the vials for 1 min in alternately liquid nitrogen and a 65 °C waterbath. After 1 h more at 45 °C and magnetic stirring, the liposomes were extruded as described above. The liposomes were then dialyzed against a buffer containing 10 mM HEPES and 150 mM NaCl (pH 7.4), using 3.5 kDa midi Pur-A-Lyzer tubes (Sigma). The dialysis was performed in two steps of 24 h with replacement of the dialysis buffer in between. In both steps, a 100-fold volume of dialysis buffer compared to the sample volume were used.

2.6. Liposome characterization

The total phosphorus concentration of the liposome stocks was determined using inductively coupled plasma mass spectrometry (ICP-MS). Samples were diluted 10000 times in an ICP-MS diluent (2% HCl, 10 ppb Ga) to fall within a set of standard samples from 25-100 ppb phosphorus, and phosphorus content was measured on an ICAP-Q from Thermo Fisher Scientific. Based on the measured

phosphorus concentrations, the lipid concentrations were estimated taking into account that cholesterol and the TriArg lipopeptide did not contain any phosphorus.

The encapsulation efficiency of the Gd-loaded liposomes was calculated by the separating liposomes from non-encapsulated DOTA(Gd) using PD10 columns and measuring the phosphorus and Gd content in the eluted fractions using ICP-MS as described above, comparing the Gd content to a standard ranging from 0.3 to 25 ppb. For all liposomes, approx. 10% of the Gd originally added to the lipid films was recovered in the final product, hereof >92.6% Gd encapsulated in the liposomes.

Hydrodynamic diameter and polydispersity (PDI) of all formulations were measured by dynamic light scattering (DLS) using a ZetaPALS from Brookhaven Instruments (Holtsville, New York, US). Liposomes were diluted to 70 µM lipid in the same sterile phosphate buffer they were also formulated in, and measurements performed as 3 runs of 30 sec at RT. The count rate was kept at 400-600 kcps. Zeta potential of the liposomes was measured using the same instrument by phase analysis light scattering (PALS) in a glucose buffer (300 mM glucose, 10 mM HEPES, 1 mM $CaCl_2$ at pH 7.4). Liposomes at a concentration of 75 µM lipid were measured with 10 runs with a target residual set to 0.04.

For imaging liposomes with cryoTEM, 3 µl of liposome solution was placed on a non-glow discharged 300 mesh copper grid with a lacey carbon support (Ted Pella, Redding, CA, US). The solution was allowed to sit for 10 sec before the excess was blotted away and plunge frozen in liquid ethane using a Vitrobot Mark IV (Thermo Fisher Scientific). Samples were imaged using a FEI Tecnai G2 20 TWIN transmission electron microscope (Thermo Fisher Scientific) operated at 200 keV in low dose mode with a FEI High-Sensitive (HS) 4k x 4k Eagle camera. Images were acquired at the Core Facility for Integrated Microscopy at University of Copenhagen.

2.7. Incubation of liposomes with whole human blood

Whole human blood (WHB) was obtained from healthy volunteers under signed content and collected in hirudin tubes (Roche Diagnostics, Mannheim, Germany). The identity of the blood donors were

unknown to the researchers involved in the study, and all requirements for blood collection at the Technical University of Denmark was followed in agreement with the guidelines of the National Committee on Health Research Ethics. The blood was added to eppendorf tubes containing liposomes pre-diluted in RPMI, giving a final liposome concentration of 500 µM total lipid. The volume percentage of WHB in the tubes was always kept above 80%. The tubes were incubated for 60 min at 37 °C with 5% CO_2 under rotation.

2.8. Flow cytometry on human leukocytes

After WHB incubation with liposomes, cells were washed 3 times in PBS containing 1% FBS. In between each wash, cells were centrifuged at 200*g* for 5 min and the supernatant discarded. In experiments with heparin washing, 3 extra washing steps with PBS containing 0.1 mg mL^{-1} (50 units mL^{-1}) heparin was introduced at this point. In each of these washing steps, samples were allowed to incubate 2-3 min with the buffer at RT before centrifugation was initiated.

Erythrocytes were lysed using BD PharmLyse lysis buffer. Four mL lysis buffer was added per 200 µL blood, followed by 15 min incubation in dark at RT. After centrifugation at 200*g* for 5 min and removal of supernatant, a second lysis with 1 mL lysis buffer for 5 min was done. Cells were washed twice in cold PBS (1% FBS) to stop the lysis. Human IgG was added to a concentration of 2 µg per 10^6 cells to block unspecific binding and incubated on ice for 10 min before transferring to a Nunc round-bottomed 96 well plate (Thermo Fischer Scientific – Nunc A/S, Roskilde, Denmark). Ten µL of APC pre-conjugated CD14 specific antibodies was added to stain monocytes and incubated on ice and in dark for 30 min. No CD14 staining was done in the experiments where CD14 had already been blocked with antibodies (see below). The plate was then spun for 8 min at 400*g* and washed with PBS twice. Finally, cells were resuspended in 100 µL PBS. Flow cytometry was performed using an ACCURI C6 flow cytometer from BD, where a minimum of 100,000 cells were acquired. APC fluorescence from the CD14 staining was measured by exciting at 640 nm and detecting at 675/25 nm (FL4). Single cells were gated in FSC-A/FSC-H plot, and cell subsets were gated using APC fluorescence and a SSC-A/FSC-A plot (see Supplementary Fig. S5). The association of liposomes

with cells was evaluated using TopFluor or DiO emission measured at 533/30 nm with excitation at 488 nm (FL1). The analysis was done in the FlowJo software.

2.9. Mouse studies

Experimental work with mice was done on 12 weeks old female BALB/cJRj mice obtained from Janvier Labs (Le Genest-Saint-Isle, France) and conducted at the Technical University of Denmark. All procedures were approved by the Danish National Animal Experiments Inspectorate. Liposomes labeled with 0.1% DiO and loaded with Gd were injected intravenously in a total volume of 125 µL in the tail vein. All liposome formulations were administered at a dose of 250 µmol/kg phospholipid, resulting in approx. 14-16 µmol/kg Gd.

2.10. Flow cytometry on murine blood samples

Sublingual blood was drawn 10 min, 30 min, 1 h, 2 h, or 4 h after injection into tubes with EDTA (final EDTA concentration ≈10 mM). For flow cytometry, aliquots of blood were taken from the 10 min and 4 h blood samples. Blood was erythrolyzed (Versalyze, Beckman Coulter, Brea, CA, US), washed in FACS buffer (0.5% BSA, 0.1% NaN_3 in PBS) and Fc-blocked (clone 2.4G2, BD Biosciences). Subsequently, all samples were stained with an eFluor780 viability dye (1:400; Thermo Fisher Scientific), 1 µg/mL BUV395 anti-mouse CD45 (clone 30-F11; BD Biosciences), 0.5 µg/mL BV785 anti-mouse Ly6c (clone HK1.4; BioLegend, San Diego, CA, US), 0.5 µg/mL PE-CF anti-mouse Ly6g (clone 1A8; BD Biosciences), 0.5 µg/mL AF647 anti-mouse CD11b (clone M1/70; BD Biosciences) for 30 min on ice in darkness. Samples were washed, fixed in 1% formaldehyde for 20 min and acquired on a BD LSRFortessa X-20 (BD Biosciences) using FACSDiva (BD Biosciences). The analysis was performed in FlowJo V10.8.1. The gating strategy is shown in Supplementary Fig. S6.

2.11. Measurement of Gd content in biological samples for PK and BD studies

Organs (liver, lung, spleen and blood) were harvested in pre-weighed 15 mL falcon tubes. The tissue was dissolved by overnight incubation in 750 µL HNO_3, 75 µL HCl and 450 µL H_2O_2 at 65 °C. The blood samples (see Section 2.10) were dissolved in 500 µL HNO_3, 50 µL HCl and 300 µL H_2O_2. All

samples were further diluted 6-100 times in 2% HCl with 10 ppb Ga, and the Gd content in the samples measured by ICP-MS on an ICAP-Q .

2.12. ELISA against complement fragments

WHB was tapped in hirudin tubes, transferred to falcon tubes and centrifuged at 1500*g* for 5 min in order to separate cells from plasma. The plasma was transferred to eppendorf tubes containing liposomes diluted in PBS to a final concentration of 1 mM total lipid. Assuming a 50% haematocrit, this concentration corresponds to the liposome concentration used in the WHB studies described above. As a positive control for complement activation, 0.2 mg/mL zymosan in MQ water was used. Pure PBS was used as negative control. The plasma was incubated under rotation for 30 min in 5% CO_2 at 37 °C. After incubation ice cold 25 mM EDTA solution was added to stop complement reactions. Tubes were spun at 21000*g* for 30 min at 4 ºC, and the supernatant was transferred to new eppendorf tubes and stored at -80 ºC until the time of running ELISA. MicroVue ELISA kits from Quidel (San Diego, CA, US) against C4d (31-A008), iC3b (31-A006), Bb (31-A027), C3a (31-A032) and sC5b9 (31-A029) were run according to manufacturer's recommendations, and absorbance measured with a Victor3 microplate reader from PerkinElmer (Waltham, MA, USA).

2.13. Inhibition studies

WHB was pre-incubated in eppendorf tubes for 30 min with or without the given inhibitor before transferring blood to the tubes with liposomes. The liposome pre-dilutions in RPMI were adjusted in order to have the same concentration of blood and liposome as in experiments without inhibitor.

The complement system was inhibited using the compstatin analog 4W9A (see above). A linear version of the peptide acquired from Tocris/Biotechne (Abingdon, UK), unable to form the disulphide bond necessary for creating the circular structure needed for the effect of the peptide, was used as control. The peptides were diluted to 360 µM in RPMI and diluted 1:9 in WHB for the pre-incubation.

The CD14 pathway was inhibited using an anti-CD14 monoclonal antibody (clone 18D11 from Hycult Biotech). The antibody was diluted in PBS to 25 µg mL^{-1} and added 1:10 to WHB. As a negative

control, the IgG1 clone MOPC-21 from Abcam (Cambridge, UK) was prepared in the same dilution. Also, pure PBS without antibody was used as negative control.

Upon pre-incubation with the various inhibitors, WHB was mixed with liposomes and incubated for 60 min at 37 °C with 5% CO_2 under rotation. Cell isolation and staining, and flow cytometry was then performed as described above.

2.14. Statistical analysis

Statistical analyses were performed using GraphPad Prism v9.0.0 (GraphPad Software, San Diego, CA, US). Error bars show standard error of mean (SEM) unless otherwise is specified. Association of liposome formulations to different cell populations (Fig. 2 and 4) were analyzed using a two-way ANOVA with Tukey's multiple comparison post hoc test. Concentration of complement proteins (Fig. 5) were compared using a two-way ANOVA with Dunnett's multiple comparison post hoc test. Inhibition effect (Fig. 6 and 7) was analyzed using a two-way ANOVA with Dunnett's multiple comparison post hoc test. The results of all statistical analyses are listed in Supplementary Table S1-S7, with references given to the relevant table in the individual figure caption.

3. Results and Discussion

3.1. Liposome characteristics

Liposomes containing the TriArg lipopeptide (Cholesterol-GWRRR) were formulated with and without PEG coating and characterized. Non-PEGylated liposomes were formulated with POPC, cholesterol and 1-3% TriArg. The zeta potentials of these liposomes were in the range of 20-40 mV (Table 1). PEGylated liposome formulations with 5% DOPE-PEG_{2000} containing POPC, cholesterol and the TriArg lipopeptide were also prepared, but to compensate for the negative charge on the DOPE anchor, the PEGylated liposomes were prepared with a higher content of TriArg (2-8%). For the PEGylated liposomes, the zeta potential reached a plateau of approximately 16-19 mV when 4% or more TriArg was added to the formulation (Table 1). Liposomes without TriArg had a slightly negative zeta potential. Liposome size was determined by DLS and ranged between 125 and 170 nm with a low polydispersity index (PDI) (Table 1). The relatively low standard deviations illustrate that the liposomes were made with high reproducibility.

Table 1. Characteristics of TriArg liposomes included in the study

Overview of the liposome formulations tested in the present study. The 30 mol% cholesterol in the formulations does not include the 1-8% cholesterol on the TriArg lipopeptide. The results are shown as the mean ± SD for all batches produced of a given formulation. Between two and seven batches were produced of each formulation.

Name	***Composition [molar ratio%] POPC:Chol:TriArg:DOPE-mPEG$_{2000}$***	***Zeta potential [mV]***	***Size [nm]***	***PDI***
0% TriArg	*70:30:0:0*	*-3.2 ±1.3*	*169.1 ±7.4*	*0.08 ±0.00*
1% TriArg	*69:30:1:0*	*19.8 ±4.0*	*145.3 ±11.7*	*0.09 ±0.02*
2% TriArg	*68:30:2:0*	*31.2 ±5.5*	*136.1 ±17.8*	*0.08 ±0.03*
3% TriArg	*67:30:3:0*	*40.5 ±3.2*	*136.6 ±16.3*	*0.06 ±0.02*
0% TriArg-PEG	*65:30:0:5*	*-8.3 ±1.4*	*129.5 ±13.1*	*0.08 ±0.01*
2% TriArg-PEG	*63:30:2:5*	*0.3 ±4.8*	*132.5 ±9.2*	*0.10 ±0.01*
3% TriArg-PEG	*62:30:3:5*	*11.9 ±2.9*	*136.7 ±0.9*	*0.16 ±0.04*
4% TriArg-PEG	*61:30:4:5*	*15.7 ±2.0*	*125.8 ±8.4*	*0.08 ±0.07*
6% TriArg-PEG	*59:30:6:5*	*19.0 ±3.5*	*126.0 ±14.6*	*0.07 ±0.03*
8% TriArg-PEG	*57:30:8:5*	*15.9 ±5.5*	*123.9 ±15.2*	*0.07 ±0.04*

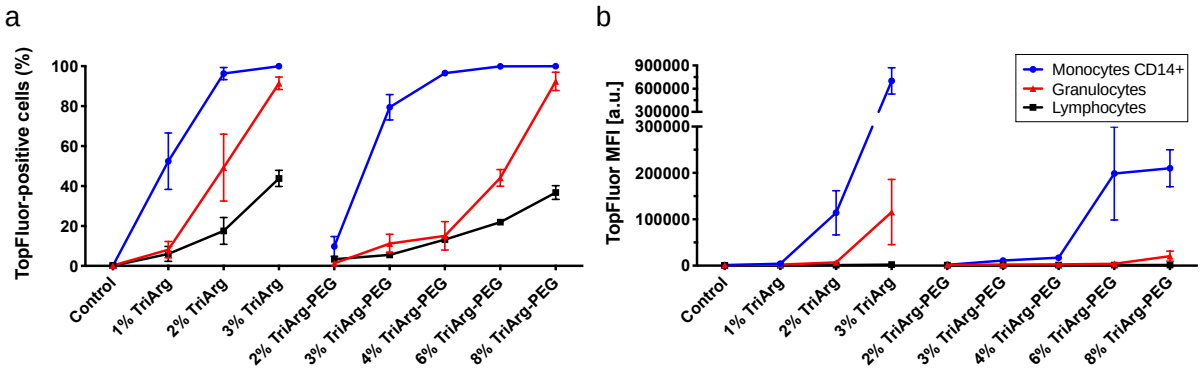

Fig. 2. Uptake of TopFluor-labeled TriArg liposomes by monocytes, granulocytes, and lymphocytes.

(a) Percentage of TopFluor-positive cells. (b) TopFluor median fluorescence intensity (MFI) of cells. At low percentages of TriArg in the formulation, the liposome uptake is highest in monocytes compared to the granulocytes and lymphocytes. The monocytes uptake further increases as TriArg content increases. At the highest percentages of TriArg tested, there is also increased uptake in granulocytes and slightly in lymphocytes. The trend is the same for PEGylated and non-PEGylated liposomes, but a higher TriArg content is required in the PEGylated liposomes to achieve the same level of cellular uptake. Error bars show SEM, and n=4 except for 3% TriArg (n=8) and 2% TriArg-PEG (n=3). A statistical analysis was carried out, and the resulting p-values for all relevant comparisons are shown in Supplementary Table S1. For gating strategy, see Supplementary Fig. S5.

To confirm the formation of vesicular structures, the liposomes were imaged using cryoTEM. As illustrated in Fig. 1c with the 6% TriArg-PEG formulation as example, the majority of the imaged liposomes were unilamellar with sizes varying from approx. 75 to 150 nm. Some of the PEGylated liposomes contained a single, smaller liposome with a size varying from 30 to 80 nm (Fig. 1c and Supplementary Fig. S7). The majority of the non-PEGylated TriArg liposomes were also unilamellar, but they co-existed with a population of multilamellar vesicles (Supplementary Fig. S8), indicating that the PEG layer ensures a more unilamellar morphology of the liposomes.

To allow tracking of the liposomes in the cellular uptake studies, all liposomes were labeled with 0.1% TopFluor-PC. To validate that the findings were independent on the choice of fluorescent lipid used to label the liposome [37], uptake experiments were also performed using liposomes formulated with an alternative fluorophore (DiO) (see Supplementary Fig. S24-26).

3.2. Cellular uptake of TriArg liposomes in whole human blood

Following formulation and characterization, the uptake of TriArg liposomes by peripheral blood leukocytes was investigated. Liposomes were incubated for 60 min with fresh WHB, and monocyte, lymphocyte and granulocyte uptake was determined by means of flow cytometry after lysis of red blood cells. Monocytes were identified based on a morphological forward/side scatter (FSC/SSC) gate and CD14 positive staining within this gate. Granulocytes and lymphocytes were identified based on morphological gates in FSC/SSC plots (Supplementary Fig. S5). The results presented in Fig. 2a demonstrate that exposure of WHB to non-PEGylated 1% TriArg liposomes resulted in liposomes associating with approximately 50% of the monocytes, whereas on average less than 10% of the granulocytes and lymphocytes exhibited liposomal uptake. When increasing the TriArg content to 2%, the uptake of the liposomes in monocytes increased to nearly 100%, whereas a more moderate increase was observed in the other cell populations. Interestingly, when comparing the median fluorescence intensity (MFI) of the monocytes exposed to the 2% TriArg liposome formulation to the MFI of the granulocytes in the same sample, a 20-fold higher MFI could be observed for the monocytes (Fig. 2b). Upon further increasing the TriArg content to 3%, the cellular uptake of the liposomes reached nearly 100% for granulocytes as well, and was about 40% for lymphocytes. Also, while the MFI increased in both monocytes and granulocytes upon treatment with the 3% TriArg liposomes, the MFI of the monocytes was only 10-fold higher than that of the granulocytes. This may overall indicate that the 2% TriArg liposomes were more selective towards monocytes compared to granulocytes and lymphocytes than liposomes with 1% TriArg or 3% TriArg.

We also investigated the leukocyte uptake of the PEGylated TriArg liposomes, using the same procedure as for the non-PEGylated liposomes. For the PEGylated liposomes, the same tendencies were observed, although at higher TriArg content: Neutrally charged 2% TriArg-PEG liposomes (zeta potential of -3.1 mV, see Table 1) were taken up by less than 20% of the monocytes, while no uptake was detected in granulocytes and lymphocytes for these liposomes. Increasing the TriArg content gradually from 2% to 6% increased liposome uptake in monocytes, both with respect to percentage of TopFluor-positive cells and the MFI (Fig. 2). However, further increasing the TriArg content to 8%, resulted in an increase in uptake by granulocytes but not by the monocytes. This indicates that the

most selective monocyte targeting for the PEGylated liposomes was achieved with 6% TriArg, whereas higher content of TriArg reduced the selectivity by increasing the off-target uptake by other cell types.

As previously discussed, the safest and most effective therapeutic outcome relies on a liposome formulation with the highest selectivity towards monocytes and the least off-target association [10,11]. We therefore assessed the monocyte targeting specificity of each formulation by calculating the ratio between the donor mean MFI of monocytes and the donor mean MFI of all remaining peripheral blood leukocytes. Fig. 3a shows the calculated specificities, which varied with the TriArg content in the liposomes. In agreement with the data in Fig. 2, the investigated formulations were generally specific to monocytes, and the TriArg content in the formulations did not correlate directly with the specificity. While the targeting specificity gives an indication of the number of liposomes per cell in monocytes versus other cell types, other recent publications have focused on the total association, which is the total number of liposomes delivered to the entire cell population [38,39]. Hence, it is highly dependent on the number of cells in each population. Despite the relatively low frequency of monocytes in blood (<5% of the blood leukocytes), the total amount of TriArg liposomes taken up by the monocytes were generally higher than the total amount taken up by all of the other leukocytes in the blood (Supplementary Fig. S9).

In a further attempt to identify a correlation between liposome characteristics and the monocyte targeting capabilities, the targeting specificity was plotted as a function of the zeta potential and net charge per 100 lipids, respectively (Fig. 3b and c). However, neither of these parameters were exclusively accountable for the targeting specificity of the investigated liposome formulations. The charge and zeta potential comparison of the TriArg and TriArg-PEG formulations indicates that PEGylation introduces a non-trivial effect with respect to biological interactions between liposomes and cells.

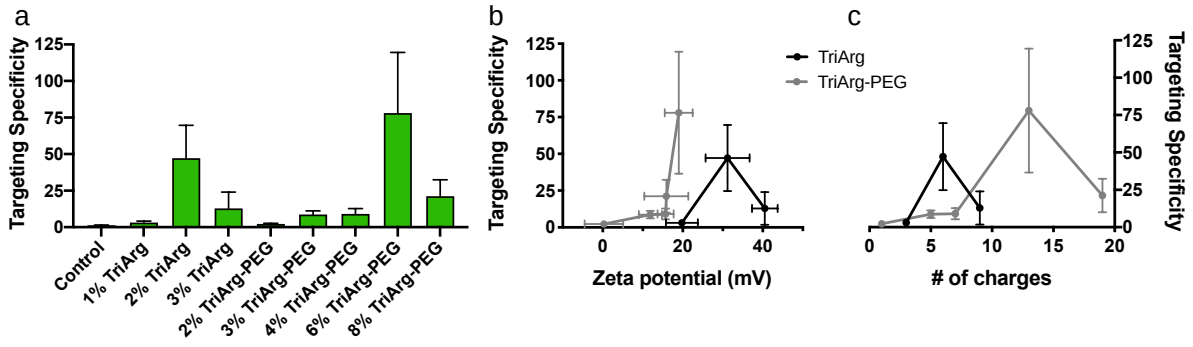

Fig. 3. Monocyte targeting specificity of TriArg liposomes.

(a) Targeting specificity of all formulations calculated by dividing the MFI of the monocyte population with the MFI of all other cells. (b) Targeting specificity as a function of zeta potential. (c) Targeting specificity as a function of the charge per 100 lipids. There is no straightforward correlation between the targeting specificity and zeta potential or the charge per 100 lipids in the formulation. The net number of charges per 100 lipids is calculated using that TriArg carries three positive charges and that DOPE-PEG carries one negative charge. Vertical error bars show SEM, and n=4 except for 3% TriArg (n=8) and 2% TriArg-PEG (n=3). Horistontal error bars show SD according to Table 1, n=2-7.

Further investigating the effect of PEGylation, we studied the stability of the liposomes in plasma using flow cytometry. It was observed that the highly charged 2% and 3% TriArg liposomes without PEGylation tended to form large aggregates when incubated in plasma (Supplementary Fig. S10-S13), whereas there was no detectable aggregation for the 1% TriArg liposomes. In comparison, the PEGylated TriArg liposomes showed higher stability – even in plasma – with almost no detectable aggregation (Supplementary Fig. S11-S13). This indicates that the PEGylated TriArg liposomes are more suitable candidates for monocyte-targeting nanocarrier therapies than the non-PEGylated TriArg liposomes.

To confirm that the liposomes were internalized by the monocytes, we tested the effect of washing the cells with heparin after liposome incubation prior to performing flow cytometry. This washing procedure is routinely used to remove unspecifically bound particles of several different types, ranging from supercharged proteins to viral peptides such as TAT and octa-arginine [40,41]. The treatment has also previously been demonstrated to remove surface-bound cationic liposomes [42,43]. As illustrated in Supplementary Fig. S14, the introduction of this washing step did not reduce the association of the liposomes with the monocytes significantly, except for the non-PEGylated 3% TriArg formulation.

The diminished association for the 3% TriArg liposomes suggests that for this formulation, the observed association is a combination of surface binding and internalization. For the remaining formulations, the data demonstrate that the MFI of the monocytes represents liposome uptake and not just association with the outer surface of the cell membrane. Similarly, the observed association with granulocytes and lymphocytes in Fig. 2 and 3 represent uptake, as illustrated in Supplementary Fig. S14. Cellular internalization of the liposomes was further confirmed by confocal microscopy, revealing the TopFluor label of the 2% TriArg liposomes appearing as intense dots inside the leukocytes (Supplementary Fig. S15). This is an advantage, as uptake of liposomes can facilitate delivery of relevant immunomodulating agents to intracellular receptors such as TLR 3, 7, 8 and 9 [29,44].

Finally, we found that the liposomes did not result in any changes in cell number, indicating low or no adverse effects of the liposomes on leukocyte viability in general and monocyte viability in particular (Supplementary Fig. S16). Neither did treatment with TriArg liposomes lead to an increase in LDH leakage from blood cells, compared to cells treated with liposome-free PBS (Supplementary Fig. S17). Together, these results indicate that the liposomes are non-toxic to blood cells.

3.3. In vivo performance of TriArg liposomes

To support our *ex vivo* findings in human blood, we also investigated the blood leukocyte uptake of TriArg liposomes *in vivo* using mice. For this experiment, 2% TriArg liposomes without PEGylation or 6% TriArg-PEG liposomes were administered intravenously. For comparison, both PEGylated and non-PEGylated liposomes without TriArg were also administered. Blood samples were collected either 10 min or 4 h after injection, and the leukocyte uptake was measured by flow cytometry tracing a DiO label on the liposomes. As shown in Fig. 4a and b, all types of liposomes were taken up by monocytes within 10 min of injection, and this uptake strongly increased by incorporation of TriArg into the formulation. Notably, there was a higher monocyte uptake of the PEGylated than of the non-PEGylated TriArg liposomes. There was only little liposome uptake by the other types of leukocytes, although the lymphocyte uptake was more prominent than neutrophil uptake *in vivo* in mice than *ex*

vivo in human blood. Overall, the data only revealed minor differences in the leukocyte uptake of the liposomes between the investigated species and between *in vivo* and *ex vivo* conditions.

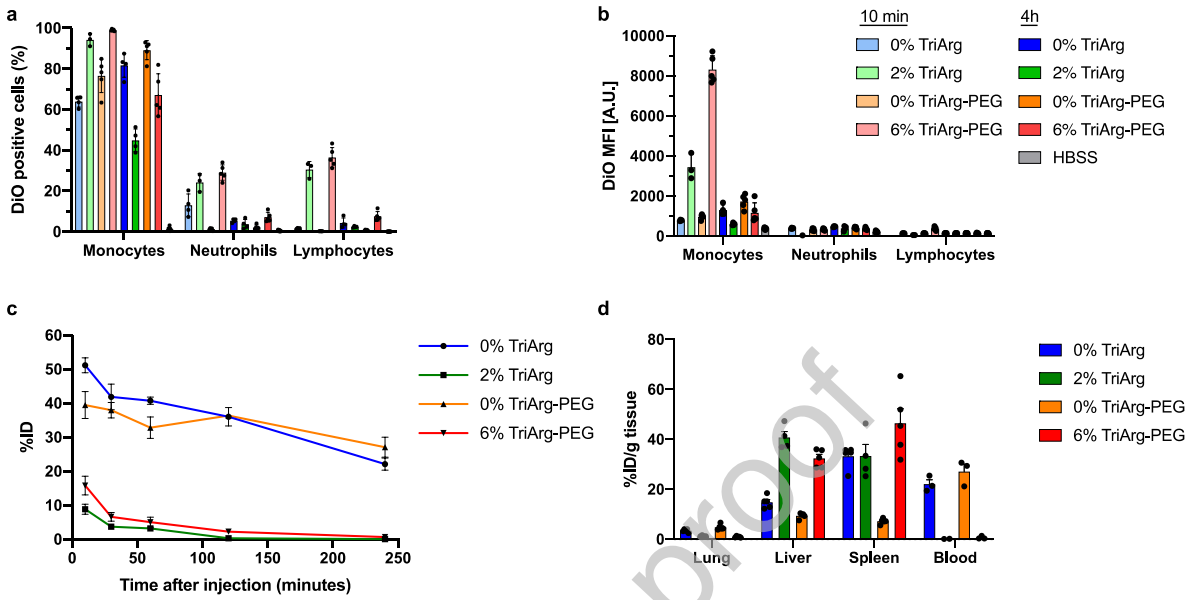

Fig. 4. Monocyte targeting of TriArg liposomes in vivo

(a) Percentage of liposome-positive cells in murine blood 10 min or 4 h after intravenous injection. (b) MFI of cell populations in murine blood 10 min or 4 h after intraveneous injection. There was a higher uptake of the liposomes in the monocytes than in the other cell populations. Inclusion of the TriArg in the liposomes further increased their uptake in monocytes. (c) Blood concentration of Gd-loaded liposomes in mice following intravenous injections. (d) Organ distribution of Gd-loaded liposomes 4 h after intraveneous injection. Incorporation of TriArg in the liposomes decreased the circulation time. More of the PEGylated than the non-PEGylated TriArg liposomes remained in circulation. Error bars show SEM. n = 3-8 for flow cytometry samples, n=5 for organ samples, n = 3 for blood samples. A statistical analysis was carried out, and the resulting p-values for all relevant comparisons are shown in Supplementary Table S2 and S3.

The association of the TriArg-containing liposomes to the monocytes decreased from the 10 min time point to the 4 h time point. To investigate this observation, we measured the pharmacokinetics and biodistribution of the four liposome formulations by loading them with gadolinium (Gd) and measuring the Gd content in the blood, liver, lungs, and spleen using ICP-MS. As shown in Fig. 4c, the TriArg liposomes were quickly cleared from circulation, although significantly more of the PEGylated than the non-PEGylated TriArg liposomes remained in the blood over the experimental time course. This could possibly be explained by the higher uptake of the PEGylated than of the non-

PEGylated TriArg liposomes in the monocytes. The biodistribution data in Fig. 4d indicate that the TriArg liposomes primarily accumulated in the liver and spleen. This could either indicate that the liposomes quickly associated to monocytes, which then immediatly left the bloodstream and travelled to the liver and spleen, or alternatively, that the liposomes travelled to the liver and spleen to directly associate with cells in these organs.

Lung accumulation has often been discussed as an artifact for cationic nanoparticles [45]. Specifically, it is hypothesized that cationic nanoparticles, including liposomes, form aggregates, which are then trapped in the lungs [46,47]. However, almost no accumulation of TriArg liposomes was observed in the lungs (Fig. 4d). Despite the tendency of the 2% TriArg liposomes to form aggregates in plasma (Supplementary Fig. S11 and S12), lung accumulation hence did not appear to be an issue.

3.4. Activation of the complement system by TriArg liposomes

In order to identify the molecular mechanism behind the observed monocyte selectivity of the TriArg liposomes, we investigated the effect of the 2% TriArg, 4% TriArg-PEG and 6% TriArg-PEG formulations on the complement system. The complement system was investigated as it is known to be involved in recognition of pathogens, nanoparticles and liposomes [48,49]. It consists of 30 soluble proteins activated by distinct pathways, recognizing various foreign surfaces [50,51]. All pathways (the classical, alternative and lectin pathways) converge on the central protein C3, which in turn has the ability to opsonize foreign substances through its cleavage product C3b/iC3b [52]. Complement activation was measured using ELISA for determining the plasma content of five different complement fragments: The anaphylatoxin C3a and the opsonin iC3b were used to measure C3 cleavage. To elucidate the pathway involved in complement activation, the C4d fragment was used to probe activation of the classical and lectin pathways, and the Bb fragment was used to determine activation of the alternative pathway. Finally, the terminal complement pathway complex was measured through analysis of the sC5b9 fragment of the Membrane Attack Complex. The concentrations of complement fragments in liposome-treated samples were normalized to the

concentrations arising from spontaneous background activation in the corresponding donor (Fig. 5). The measured concentration of the fragments can be found in Supplementary Fig. S18.

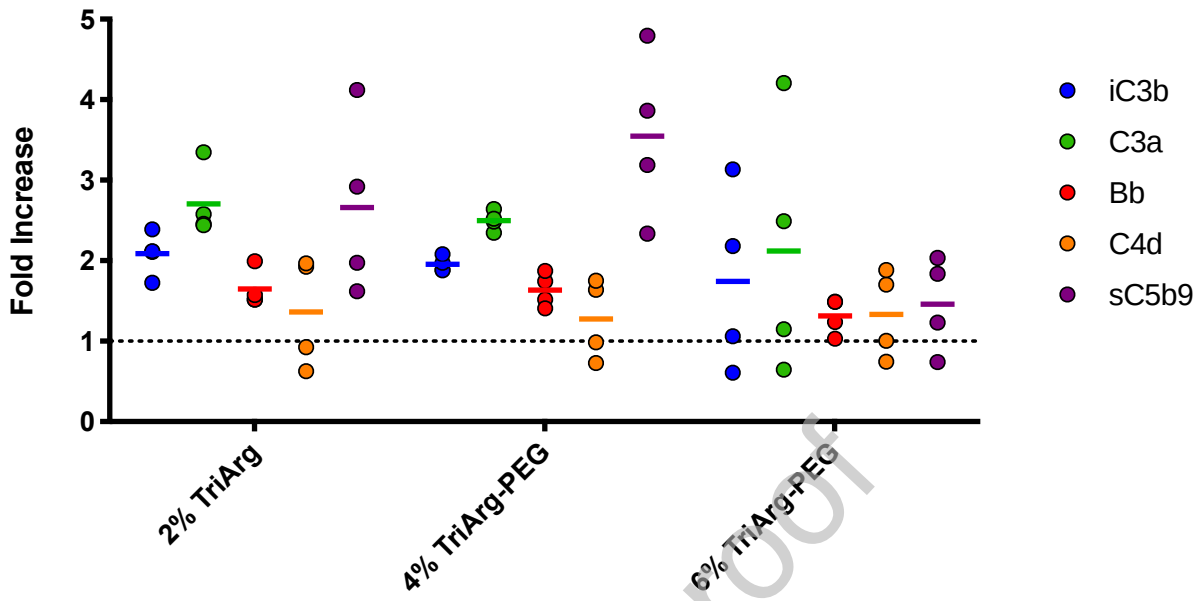

Fig. 5. Complement activation increase in plasma upon exposure to TriArg liposomes

Concentration of complement fragment in plasma normalized to the control sample for every single donor, giving the fold increase in concentration of each complement fragment upon exposure of plasma to liposomes. Concentrations of complement fragments C3a and iC3b increase over the background when exposed to 2% TriArg and 4% TriArg-PEG liposomes, indicating that the complement system is activated. Comparing the increase in Bb (alternative pathway) and C4d fragments (classical or lectin pathway) indicates that the activation is through the alternative pathway. An increase in sC5b9 show that the terminal pathways of complement is also initiated. The 6% TriArg-PEG liposomes do not give rise to a significant increase in concentration for any of the complement fragments tested. n=4, error bars show SEM. A statistical analysis was carried out, and the resulting p-values for all relevant comparisons are shown in Supplementary Table S4.

In agreement with previously published results, the data in Fig. 5 demonstrate that activation of the complement system by the liposomes was highly donor dependent [53]. Specifically, the data demonstrate that the 2% TriArg and 4% TriArg-PEG formulations activate the alternative pathway of the complement system, as evident by a general increase in all donors for C3a, iC3b and Bb. On the other hand, the concentration of the C4d fragment was unaffected in two of the four donors and increased two-fold in the two other donors, indicating activation of the classical pathway in these two donors. The increase in the sC5b9 fragment for the 2% TriArg and 4% TriArg-PEG formulations suggests formation of the membrane attack complex. In case of the 6% TriArg-PEG liposomes, activation of complement was more irregular. While two donors did not respond to the treatment, the

classical pathway was activated in the other two donors, as seen by an increase in C3a, iC3b, C4d and to some extent sC5b9.

Overall, there were no obvious correlations between complement activation properties and the TriArg content, zeta potential, or uptake properties of the liposomes. Of the three liposomes investigated, the only one not showing a significant increase in complement activation, the 6% TriArg-PEG formulation, was the most specific to monocytes (Fig. 3a) as well as the one with the highest monocyte uptake (Fig. 2b). To further explore these observations, the effect on the monocyte uptake when the complement system was inhibited was investigated.

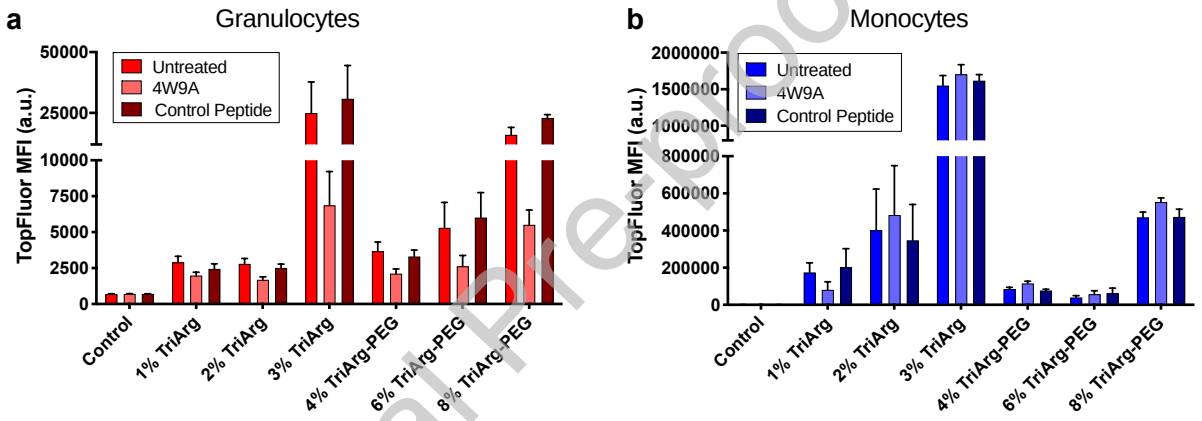

Fig. 6. Uptake of TriArg liposomes in leukocytes upon inhibition of the complement system

The complement system in fresh whole human blood was inhibited using the compstatin-analog 4W9A before adding liposomes and investigating leukocyte uptake by flow cytometry. Uptake of liposomes in granulocytes (a) and monocytes (b) upon pre-incubation of blood with either complement inhibitor 4W9A or an inactive linear control peptide. The 4W9A peptide reduces the liposome uptake in the granulocytes, but not in the monocytes or lymphocytes. n=4, error bars show SEM. A statistical analysis was carried out, and the resulting p-values for all relevant comparisons are shown in Supplementary Table S5.

3.5. Cellular uptake of TriArg liposomes upon inhibition of the complement system

Complement inhibition studies were performed by blocking C3 cleavage, thus preventing formation of the cleavage product C3b which can otherwise opsonize liposomes and drive their cellular uptake. The clinically approved cyclic peptide compstatin can protect C3 from enzymatic cleavage [54]. Here, we inhibited C3 cleavage by pre-incubating WHB for 30 min with the compstatin analog 4W9A, which is 45-fold more potent than the parental peptide [55], before adding the liposomes to the blood. As a

negative control, the blood was pre-treated with a linear inactive control peptide of comparable sequence to compstatin. This strategy for inhibition of complement is much more specific and precise than, for example, heat treatment of serum or addition of EDTA, two popular alternatives for inhibition of complement [56,57]. Liposome uptake was evaluated with flow cytometry, as described above. The ability of 4W9A to inhibit complement activation (and the lack of inhibition by the control peptide) is demonstrated in a proof of concept assay in Supplementary Fig. S19.

The uptake in granulocytes and monocytes upon complement inhibition is shown in Fig. 6a and b, respectively. Compared to untreated blood or blood pre-incubated with the control peptide, pre-treatment with 4W9A decreased liposome uptake in granulocytes irrespective of formulation. Interestingly, the decrease correlated with the TriArg content of the liposomes, so the highest inhibitory effect was observed for liposomes formulated with a high percentage of TriArg, both in the case of non-PEGylated and PEGylated liposomes (Supplementary Fig. S20). In contrast, 4W9A treatment did not generally reduce the uptake in the monocytes (Fig. 6b), but actually showed a trend towards a slight increase in monocyte uptake. This is supported by the results in Supplementary Fig. S20 showing that 4W9A inhibition does not decrease the monocyte targeting specificity, but rather trends towards an increase in monocyte targeting specificity. Consequently, we conclude that the complement system is not the mechanism responsible for the monocyte targeting of the TriArg liposomes; instead, the complement system is involved in the mechanism of uptake in granulocytes. This mirrors earlier studies, finding that neutrophil uptake of liposomes is mediated by the complement system [39,58].

The complement system-mediated off-target uptake in granulocytes could potentially explain the differences in monocyte uptake *ex vivo* in human blood and *in vivo* in mouse blood. In human blood, the granulocyte uptake was second-highest, only surpassed by monocytes, whereas in mouse blood, the granulocyte uptake was lower than in lymphocytes. This could be explained by differences in the complement system between mice and human.[59–61]

3.6. Cellular uptake of TriArg liposomes upon CD14 blockade

In a further attempt to identify the mechanism governing the monocyte targeting of TriArg liposomes, the CD14 pathway was investigated. The membrane-bound version of the CD14 receptor (mCD14) has, in addition to being a differentiation marker for monocytes, been shown to be involved in signaling in response to cationic liposomes [62,63]. To test the potential involvement of CD14, WHB was pre-incubated for 30 min with either a CD14-blocking antibody (clone 18D11) or an unspecific isotype antibody prior to liposome incubation for 60 min and subsequent assessment of uptake by flow cytometry.

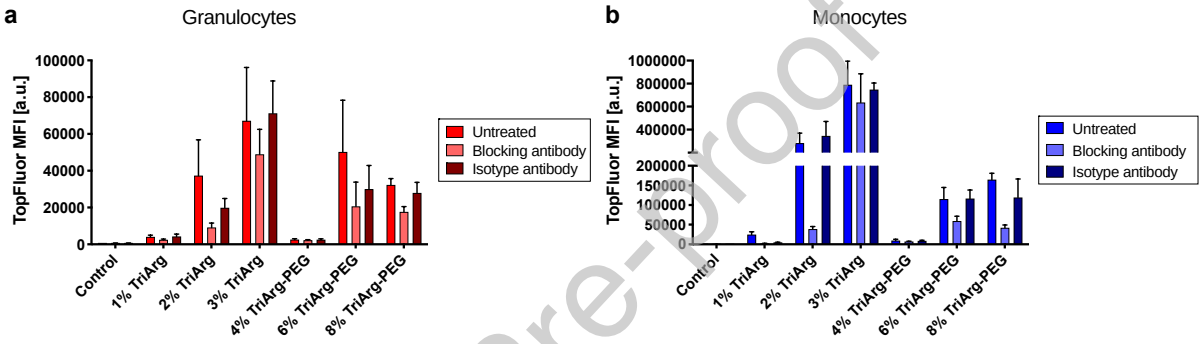

Fig. 7. Inhibition of cellular uptake of TriArg liposomes with a CD14 blocking antibody.

Uptake of liposomes in granulocytes (a) and monocytes (b) upon pre-incubation of blood with either CD14-blocking antibody (clone 18D11) or an isotype antibody (clone MOPC21), as well as in the absence of any antibodies. n=4 except for 2% TriArg and 6% TriArg-PEG with n=6. Error bars show SEM. A statistical analysis was carried out, and the resulting p-values for all relevant comparisons are shown in Supplementary Table S6.

We investigated the uptake of the TriArg liposomes in both granulocytes and monocytes upon treatment with a CD14-blocking antibody (Fig. 7). The monocyte uptake was drastically reduced for the non-PEGylated 2% TriArg liposomes, as well as for the 6% TriArg-PEG and 8% TriArg-PEG liposomes in blood pre-treated with the CD14-blocking antibody compared to untreated blood and blood pre-treated with an isotype antibody (Fig. 7b). The granulocyte uptake for the same liposomes was also reduced upon CD14 blockade, but only to a lesser extent (Fig. 7a and Supplementary Fig. S21). Consequently, the monocyte targeting specificity was found to decrease for the liposomes upon blockade of CD14 (Supplementary Fig. S21). The extent of inhibition was dependent on the antibody concentration, again being most pronounced in monocytes followed by granulocytes, but with little

effect on lymphocyte uptake (Supplementary Fig. S22). This strongly suggests the involvement of CD14 in the uptake mechanism of the TriArg liposomes. Worth noting, the 3% TriArg formulation, which exhibited a high uptake in both the granulocytes and monocytes, was less affected by the blockade of CD14. However, as mentioned above, these liposomes formed aggregates in plasma (Supplementary Fig. S11). Ahl *et al.* demonstrated that size and aggregation is an important determinant for liposome clearance, independent on opsonization of the liposomes [64]. Accordingly, aggregation could potentially explain the inconsistent behavior we observed for the 3% TriArg liposomes.

To further support the role of the CD14 pathway in monocyte targeting, we also inhibited the LPS Binding Protein (LBP), which is upstream of CD14 (Fig. 8) in the TLR4 response to bacterial lipids [65], using the inhibitor sesamol. As shown in Supplementary Fig. S23 we observed an inhibition similar to the one with the CD14-blocking antibody, being most effective in monocytes, less pronounced in granulocytes and with limited effect in lymphocytes.

Based on the above data, we propose that the monocyte specificity is in part mediated by the CD14 pathway. While mCD14 was originally assumed to be exclusively expressed on monocytes, it is today accepted that the receptor is also weakly expressed on other cell types, e.g. neutrophils that make up the vast majority of the granulocytes [66]. Furthermore, a soluble version of the CD14 receptor (sCD14) can also mediate uptake in other cell types than monocytes, and sCD14 is believed to be secreted by monocytes in order to help other types of peripheral blood leukocytes in clearing LPS and other lipids [66]. It is thus logical that CD14 (both in membrane-bound and soluble form) is not solely involved in monocyte uptake, but also in the uptake in other cell types.

It is not clear if the pathway dependency is related to the cationic charge of TriArg alone or whether it has to do with the structure of the TriArg lipopeptide being a specific ligand for CD14. In any case, monocyte uptake [21] and stimulation of inflammatory pathways [63] by cationic particles has indeed been observed for other cationic lipids, but variations in the immune responses of different lipids

suggest that different mechanisms are in play [67]. Alternative pathways including scavenger receptors, integrins as well as antibody-mediated routes may thus also play a role in clearance of the TriArg liposomes. Future studies might reveal the role of CD14 in uptake of other liposomes formulated with different cationic lipids. Interestingly, charge targeting can also be used to target other peripheral blood leukocyte populations than monocytes, as anionic liposomes have been demonstrated to primarily associate to neutrophils in mouse blood [39]. Importantly, the neutrophil targeting capacities were found to depend on the activation state of the cells, as enhanced neutrophil uptake was observed upon LPS pre-stimulation of the mice. The authors also observed that LPS pre-stimulation resulted in increased monocyte-association of cationic liposomes in mouse blood [39]. Future investigations may reveal if inflammation will also enhance the monocyte-targeting capabilities of cationic liposomes in blood from human donors.

3.7. Proposed mechanism of uptake

It has previously been illustrated how cationic liposomes trigger CD14-mediated signaling processes in immune cells [63]. As mentioned above, the CD14 protein exists both in a membrane-bound version (mCD14) and in a soluble version (sCD14). CD14 was originally identified as being a TLR co-receptor, accountable for controlling the TLR4 mediated response to LPS: In the absence of CD14, TLR4 is located at the plasma membrane even when engaged in signaling; in the presence of CD14, the receptor complex is endocytosed when activated, see Fig. 8 [65,68]. CD14 has also been shown to be involved in intracellular signaling in response to cationic lipids [63,69], in endocytosis of dead cell components [70], in extracellular trafficking of several types of phospholipids [71], and to mediate signaling and uptake through other receptors, such as CR3 and TLR2 [69,72]. Based on this knowledge, taken together with the data on complement-, CD14- and LBP-inhibition presented in this work, we propose the uptake mechanisms illustrated in Fig. 8 for the liposome formulations investigated in the current work.

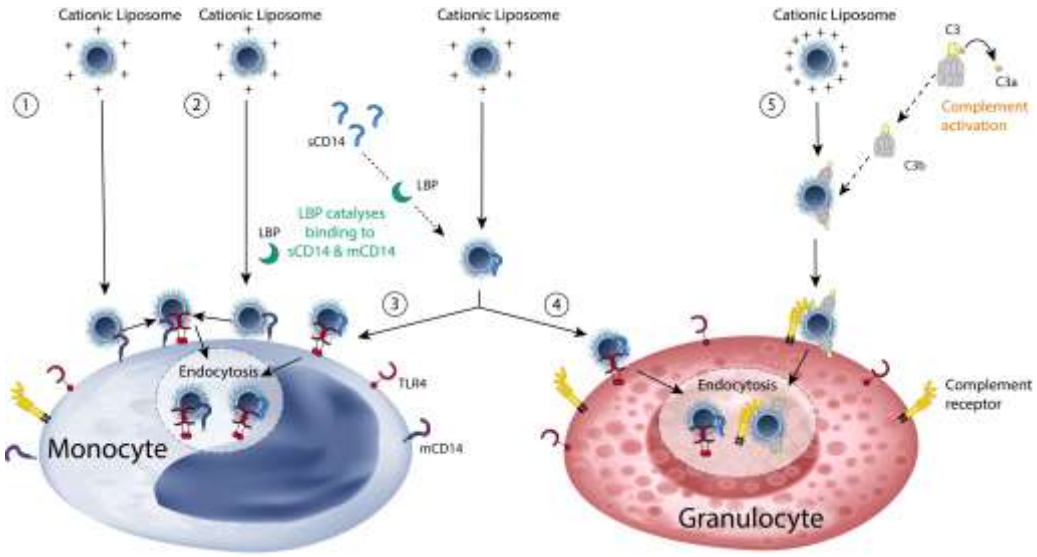

Fig. 8. Proposed pathway for uptake of TriArg liposomes through the CD14 receptor.

CD14 exists both as a membrane bound version (mCD14) and as a soluble version (sCD14). The former is primarily expressed on monocytes, and can thus directly facilitate uptake in monocytes (1). TLR4 signaling, e.g. in response to LPS on gram-negative bacteria, usually happens with the receptor being located at the plasma membrane [65,68]. *The TLR4 receptor alone is not able to bind LPS directly, but needs an accessory protein* [68]. *When this accessory protein is CD14, TLR4 in complex with the ligand is endocytosed, instead of being located at the membrane* [68,69]. *The CD14/TLR-4 complex can in this way facilitate internalization of the bacteria* [73], *apoptotic cells* [74], *or other lipid particles recognized by CD14, e.g. the cationic liposomes presented here. CD14 can directly bind LPS on gram-negative bacteria, PS on apoptotic cells, and a range of other lipids, but the LPS Binding Protein (LBP) can promote this binding (2)* [71,75,76], *thereby enhancing the TLR4 activation in response to LPS 100-1000 fold compared to serum without LBP. In addition, LBP is involved in CD14-mediated phagocytosis* [73]. *Furthermore, the soluble version of CD14, sCD14, can facilitate uptake in both monocytes (3) and non-myeloid cells such as granulocytes (4). The figure illustrates how CD14 could thus serve as a co-receptor driving endocytosis of cationic liposomes in both CD14 positive monocytes and in cells with low or none mCD14 expression. It should be noted, that a low degree of mCD14 expression in granulocytes could also mediate uptake in these cells in parallel to the complement-mediated opsonization. The results presented in this paper supports that this LBP/CD14-pathway, previously demonstrated for monocyte phagocytosis of bacteria* [73], *is also involved in uptake of cationic liposomes. In parallel, however, the complement system can also facilitate uptake in granulocytes (5). This pathway seems to dominate when the TriArg content is increased (see data in Fig. 7).*

4. Conclusion:

We have demonstrated that the cationic TriArg liposomes designed in this study are taken up specifically by monocytes in WHB *ex vivo* and in mouse blood *in vivo*. PEGylation improved the stability of the liposomes by efficiently preventing aggregation in plasma, without compromising their

targeting capacity. The selective monocyte uptake of the liposomes renders them as promising tools in stimulating the activation and differentiation of monocytes by means of delivering immunostimulants.

Precise understanding of how immune cell targeting can be achieved through natural immune mechanisms is essential for developing directed vaccines and immune modulating therapies within cancer, infectious and autoimmune diseases. In line with this, the current study illuminates important mechanisms underlying monocyte targeting and establishes that while the targeting to monocytes is mediated by the CD14 pathway, the complement system is activated by the TriArg liposomes and results in off-target uptake in granulocytes. These findings represent an important step forward in achieving in-depth mechanistic understanding that ultimately aids rational design of directed vaccines.

Supplementary Material.

Supplementary figures associated with this article can be found in the online version of the paper.

Acknowledgements

The authors would like to acknowledge Jannik Pedersen for helping with blood sampling, Fredrik Melander for carrying out the ICP-MS measurements, and Ellen Vallentin Asmus and Nanna Bild for helping with the figures. Additionally, the authors would like to acknowledge Doha Grannam, Aristeidis Koukos, Matilde Smærup Jørgensen, Unnur Jóna Björgvinsdóttir and Tsinat Berhane for assistance with the mouse study.

Funding

This works was supported by The Lundbeck Foundation (Grant number R155-2013-14113), the European Research Council (Grant number ERC 310985), the Novo Nordisk Foundation (Grant number NNF16OC0022166), and the Danish Council for Independent Research (Grant number DFF 4184-00514). The funding sources did not have impact on the design, interpretation or reporting of the study.

Disclosure:

T.L. Andresen, L. Parhamifar and R. Münter have IP on cationic liposomes for immunotherapy (Patent number WO2019012107). The authors declare no other relevant affiliations with financial interests.

References:

[1] D.C. Wraith, The Future of Immunotherapy: A 20-Year Perspective, Front. Immunol. 8 (2017). doi:10.3389/fimmu.2017.01668.

[2] A. Schroeder, D.A. Heller, M.M. Winslow, J.E. Dahlman, G.W. Pratt, R. Langer, T. Jacks, D.G. Anderson, Treating metastatic cancer with nanotechnology, Nat. Rev. Cancer. 12 (2012) 39–50. doi:10.1038/nrc3180.

[3] I. Mellman, G. Coukos, G. Dranoff, Cancer immunotherapy comes of age, Nature. 480 (2011) 480–489.

[4] M. Feldmann, L. Steinman, Design of effective immunotherapy for human autoimmunity, Nature. 435 (2005) 612–619. doi:10.1038/nature03727.

[5] R.M. Steinman, M. Pope, Exploiting dendritic cells to improve vaccine efficacy, J. Clin. Invest. 109 (2002) 1519–1526. doi:10.1172/JCI0215962.

[6] K. Palucka, J. Banchereau, Cancer immunotherapy via dendritic cells, Nat. Cancer. 12 (2012) 265–277.

[7] M. Saxena, S.H. van der Burg, C.J.M. Melief, N. Bhardwaj, Therapeutic cancer vaccines, Nat. Rev. Cancer. 21 (2021) 360–378. doi:10.1038/s41568-021-00346-0.

[8] E. Karathanasis, C.M. Geigerman, C.A. Parkos, L. Chan, R. V. Bellamkonda, D.L. Jaye, Selective targeting of nanocarriers to neutrophils and monocytes, Ann. Biomed. Eng. 37 (2009) 1984–1992. doi:10.1007/s10439-009-9702-5.

[9] C. Kelly, C. Jefferies, S.-A. Cryan, Targeted Liposomal Drug Delivery to Monocytes and Macrophages, J. Drug Deliv. 2011 (2011) 1–11. doi:10.1155/2011/727241.

[10] S. Basith, B. Manavalan, T.H. Yoo, S.G. Kim, S. Choi, Roles of toll-like receptors in Cancer: A double-edged sword for defense and offense, Arch. Pharm. Res. 35 (2012) 1297–1316. doi:10.1007/s12272-012-0802-7.

[11] J. Damm, F. Wiegand, L.M. Harden, R. Gerstberger, C. Rummel, J. Roth, Fever, sickness behavior, and expression of inflammatory genes in the hypothalamus after systemic and localized subcutaneous stimulation of rats with the toll-like receptor 7 agonist imiquimod, Neuroscience. 201 (2012) 166–183. doi:10.1016/j.neuroscience.2011.11.013.

[12] E. Sayour, H. Mendez-Gomez, D. Mitchell, Cancer Vaccine Immunotherapy with RNA-Loaded Liposomes, Int. J. Mol. Sci. 19 (2018) 2890. doi:10.3390/ijms19102890.

[13] S.T. Koshy, A.S. Cheung, L. Gu, A.R. Graveline, D.J. Mooney, Liposomal Delivery Enhances Immune Activation by STING Agonists for Cancer Immunotherapy, Adv. Biosyst. 1 (2017) 1600013. doi:10.1002/adbi.201600013.

[14] P. Zamani, A.A. Momtazi-Borojeni, M.E. Nik, R.K. Oskuee, A. Sahebkar, Nanoliposomes as the adjuvant delivery systems in cancer immunotherapy, J. Cell. Physiol. 233 (2018) 5189–5199. doi:10.1002/jcp.26361.

[15] E.M. Varypataki, K. van der Maaden, J. Bouwstra, F. Ossendorp, W. Jiskoot, Cationic

Liposomes Loaded with a Synthetic Long Peptide and Poly(I:C): a Defined Adjuvanted Vaccine for Induction of Antigen-Specific T Cell Cytotoxicity, AAPS J. 17 (2015) 216–226. doi:10.1208/s12248-014-9686-4.

[16] L.N. Ramana, S. Sharma, S. Sethuraman, U. Ranga, U.M. Krishnan, Investigation on the stability of saquinavir loaded liposomes: Implication on stealth, release characteristics and cytotoxicity, Int. J. Pharm. 431 (2012) 120–129. doi:10.1016/j.ijpharm.2012.04.054.

[17] G. Bozzuto, A. Molinari, Liposomes as nanomedical devices, Int. J. Nanomedicine. 10 (2015) 975. doi:10.2147/IJN.S68861.

[18] S. Mallick, J.S. Choi, Liposomes: Versatile and Biocompatible Nanovesicles for Efficient Biomolecules Delivery, J. Nanosci. Nanotechnol. 14 (2014) 755–765. doi:10.1166/jnn.2014.9080.

[19] R.A. Schwendener, Liposomes as vaccine delivery systems: A review of the recent advances, Ther. Adv. Vaccines. (2014). doi:10.1177/2051013614541440.

[20] D. Chatzikleanthous, D.T. O'Hagan, R. Adamo, Lipid-Based Nanoparticles for Delivery of Vaccine Adjuvants and Antigens: Toward Multicomponent Vaccines, Mol. Pharm. 18 (2021) 2867–2888. doi:10.1021/acs.molpharmaceut.1c00447.

[21] P.T. Johansen, D. Zucker, L. Parhamifar, H. Pourhassan, D.V. Madsen, J.R. Henriksen, M. Gad, A. Barberis, R. Maj, T.L. Andresen, S.S. Jensen, Monocyte targeting and activation by cationic liposomes formulated with a TLR7 agonist, Expert Opin. Drug Deliv. 12 (2015) 1045–1058. doi:10.1517/17425247.2015.1009444.

[22] D.M. Copolovici, K. Langel, E. Eriste, Ü. Langel, Cell-Penetrating Peptides: Design, Synthesis, and Applications, ACS Nano. 8 (2014) 1972–1994. doi:10.1021/nn4057269.

[23] N. Schmidt, A. Misra, G.H. Lai, G.C. Wong, Arginine-rich cell-penetrating peptides, FEBS Lett. 584 (2010) 1806–1813.

[24] R. Brock, The Uptake of Arginine-Rich Cell-Penetrating Peptides: Putting the Puzzle Together, Bioconjug. Chem. 25 (2014) 863–868. doi:10.1021/bc500017t.

[25] A. Liberska, A. Unciti-Broceta, M. Bradley, Very long-chain fatty tails for enhanced transfection, Org. Biomol. Chem. 7 (2009) 61–68. doi:10.1039/B815733B.

[26] C. Allolio, A. Magarkar, P. Jurkiewicz, K. Baxová, M. Javanainen, P.E. Mason, R. Šachl, M. Cebecauer, M. Hof, D. Horinek, V. Heinz, R. Rachel, C.M. Ziegler, A. Schröfel, P. Jungwirth, Arginine-rich cell-penetrating peptides induce membrane multilamellarity and subsequently enter via formation of a fusion pore, Proc. Natl. Acad. Sci. 115 (2018) 11923–11928. doi:10.1073/pnas.1811520115.

[27] M. Di Pisa, G. Chassaing, J.-M. Swiecicki, Translocation Mechanism(s) of Cell-Penetrating Peptides: Biophysical Studies Using Artificial Membrane Bilayers, Biochemistry. 54 (2015) 194–207. doi:10.1021/bi501392n.

[28] F. Madani, S. Lindberg, Ü. Langel, S. Futaki, A. Gräslund, Mechanisms of Cellular Uptake of

Cell-Penetrating Peptides, J. Biophys. (2011). doi:10.1155/2011/414729.

[29] E.L.J.M. Smits, P. Ponsaerts, Z.N. Berneman, V.F.I. Van Tendeloo, The Use of TLR7 and TLR8 Ligands for the Enhancement of Cancer Immunotherapy, Oncologist. 13 (2008) 859–875. doi:10.1634/theoncologist.2008-0097.

[30] H.A. Rydberg, M. Matson, H.L. Åmand, E.K. Esbjörner, B. Nordén, Effects of Tryptophan Content and Backbone Spacing on the Uptake Efficiency of Cell-Penetrating Peptides, Biochemistry. 51 (2012) 5531–5539. doi:10.1021/bi300454k.

[31] A. Ziegler, J. Seelig, Contributions of Glycosaminoglycan Binding and Clustering to the Biological Uptake of the Nonamphipathic Cell-Penetrating Peptide WR 9, Biochemistry. 50 (2011) 4650–4664. doi:10.1021/bi1019429.

[32] C. Bechara, M. Pallerla, Y. Zaltsman, F. Burlina, I.D. Alves, O. Lequin, S. Sagan, Tryptophan within basic peptide sequences triggers glycosaminoglycan-dependent endocytosis, FASEB J. 27 (2013) 738–749. doi:10.1096/fj.12-216176.

[33] M.-L. Jobin, M. Blanchet, S. Henry, S. Chaignepain, C. Manigand, S. Castano, S. Lecomte, F. Burlina, S. Sagan, I.D. Alves, The role of tryptophans on the cellular uptake and membrane interaction of arginine-rich cell penetrating peptides, Biochim. Biophys. Acta - Biomembr. 1848 (2015) 593–602. doi:10.1016/j.bbamem.2014.11.013.

[34] D. V. Devine, A.J. Bradley, The complement system in liposome clearance: Can complement deposition be inhibited?, Adv. Drug Deliv. Rev. 32 (1998) 19–29. doi:10.1016/S0169-409X(97)00129-4.

[35] A. Francian, K. Mann, M. Kullberg, Complement C3-dependent uptake of targeted liposomes into human macrophages, B cells, dendritic cells, neutrophils, and MDSCs, Int. J. Nanomedicine. Volume 12 (2017) 5149–5161. doi:10.2147/IJN.S138787.

[36] R.L. Juliano, Factors affecting the clearance kinetics and tissue distribution of liposomes, microspheres and emulsions, Adv. Drug Deliv. Rev. 2 (1988) 31–54. doi:10.1016/0169-409X(88)90004-X.

[37] R. Münter, K. Kristensen, D. Pedersbæk, J.B. Larsen, J.B. Simonsen, T.L. Andresen, Dissociation of fluorescently labeled lipids from liposomes in biological environments challenges the interpretation of uptake studies, Nanoscale. 10 (2018) 22720–22724. doi:10.1039/C8NR07755J.

[38] Y.R. Ong, R. De Rose, A.P.R. Johnston, In Vivo Quantification of Nanoparticle Association with Immune Cell Subsets in Blood, Adv. Healthc. Mater. 10 (2021) 2002160. doi:10.1002/adhm.202002160.

[39] S. Li, M. Li, S. Huo, Q. Wang, J. Chen, S. Ding, Z. Zeng, W. Zhou, Y. Wang, J. Wang, Voluntary-Opsonization-Enabled Precision Nanomedicines for Inflammation Treatment, Adv. Mater. 33 (2021) 2006160. doi:10.1002/adma.202006160.

[40] M. Lundberg, S. Wikström, M. Johansson, Cell surface adherence and endocytosis of protein

transduction domains, Mol. Ther. 8 (2003) 143–150. doi:10.1016/S1525-0016(03)00135-7.

[41] B.R. McNaughton, J.J. Cronican, D.B. Thompson, D.R. Liu, Mammalian cell penetration, siRNA transfection, and DNA transfection by supercharged proteins, PNAS. 106 (2009) 611–6116.

[42] K. Smith Korsholm, E.M. Agger, C. Foged, D. Christensen, J. Dietrich, C.S. Andersen, C. Geisler, P. Andersen, The adjuvant mechanism of cationic dimethyldioctadecylammonium liposomes, Immunology. 121 (2007) 216–226. doi:10.1111/j.1365-2567.2007.02560.x.

[43] A. Iwasa, H. Akita, I. Khalil, K. Kogure, S. Futaki, H. Harashima, Cellular uptake and subsequent intracellular trafficking of R8-liposomes introduced at low temperature, Biochim. Biophys. Acta - Biomembr. 1758 (2006) 713–720. doi:10.1016/j.bbamem.2006.04.015.

[44] S. Dow, Liposome–nucleic acid immunotherapeutics, Expert Opin. Drug Deliv. 5 (2008) 11–24. doi:10.1517/17425247.5.1.11.

[45] L. Liu, Y. Liu, B. Xu, C. Liu, Y. Jia, T. Liu, C. Fang, W. Wang, J. Ren, Z. He, K. Men, X. Liang, M. Luo, B. Shao, Y. Mao, H. Xiao, Z. Qian, J. Geng, B. Dong, P. Mi, Y. Jiang, Y. Wei, X. Wei, Negative regulation of cationic nanoparticle-induced inflammatory toxicity through the increased production of prostaglandin E2 via mitochondrial DNA-activated Ly6C + monocytes, Theranostics. 8 (2018) 3138–3152. doi:10.7150/thno.21693.

[46] H. Skovgaard Poulsen, Arildsen, J. Roth, H. Skovgaard Poulsen, Tuxen Poulsen, Christensen, Handlos, T. Gjetting, In vitro and in vivo effects of polyethylene glycol (PEG)-modified lipid in DOTAP/cholesterol-mediated gene transfection, Int. J. Nanomedicine. (2010) 371. doi:10.2147/IJN.S10462.

[47] Y. Maitani, Nakamura, Kon, Sumiyoshi, Fujine, Kogiso, Shimizu, Asakawa, Sanada, Higher lung accumulation of intravenously injected organic nanotubes, Int. J. Nanomedicine. (2013) 315. doi:10.2147/IJN.S38462.

[48] M.A. Dobrovolskaia, P. Aggarwal, J.B. Hall, S.E. McNeil, Preclinical Studies To Understand Nanoparticle Interaction with the Immune System and Its Potential Effects on Nanoparticle Biodistribution, Mol. Pharm. 5 (2008) 487–495. doi:10.1021/mp800032f.

[49] S.M. Moghimi, I. Hamad, Liposome-Mediated Triggering of Complement Cascade, J. Liposome Res. 18 (2008) 195–209.

[50] N.S. Merle, R. Noe, L. Halbwachs-Mecarelli, V. Fremeaux-Bacchi, L.T. Roumenina, Complement System Part II: Role in Immunity, Front. Immunol. 6 (2015). doi:10.3389/fimmu.2015.00257.

[51] N.S. Merle, S.E. Church, V. Fremeaux-Bacchi, L.T. Roumenina, Complement System Part I: Molecular Mechanisms of Activation and Regulation, Front. Immunol. 6 (2015). doi:10.3389/fimmu.2015.00262.

[52] X. Yan, G.L. Scherphof, J.A.A.M. Kamps, Liposome Opsonization, J. Liposome Res. 15 (2005) 109–139. doi:10.1081/LPR-64971.

[53] H. Benasutti, G. Wang, V.P. Vu, R. Scheinman, E. Groman, L. Saba, D. Simberg, Variability of Complement Response toward Preclinical and Clinical Nanocarriers in the General Population, Bioconjug. Chem. 28 (2017) 2747–2755. doi:10.1021/acs.bioconjchem.7b00496.

[54] D.C. Mastellos, D. Yancopoulou, P. Kokkinos, M. Huber-Lang, G. Hajishengallis, A.R. Biglarnia, F. Lupu, B. Nilsson, A.M. Risitano, D. Ricklin, J.D. Lambris, Compstatin: a C3-targeted complement inhibitor reaching its prime for bedside intervention, Eur J Clin Invest. 45 (2015) 423–440.

[55] B. Mallik, M. Katragadda, L.A. Spruce, C. Carafides, C.G. Tsokos, D. Morikis, J.D. Lambris, Design and NMR Characterization of Active Analogues of Compstatin Containing Non-Natural Amino Acids, J. Med. Chem. 48 (2005) 274–286. doi:10.1021/jm0495531.

[56] A. Kandus, M. Benedik, A.F. Bren, J. Drinovec, D. Fliser, B. Knap, S. Kladnik, P. Ivanovich, Inhibition of complement activation with EDTA in vivo during sham hemodialysis, Int. J. Artif. Organs. (1991). doi:10.1177/039139889101400810.

[57] R.D. Soltis, D. Hasz, M.J. Morris, I.D. Wilson, The effect of heat inactivation of serum on aggregation of immunoglobulins., Immunology. (1979).

[58] J.W. Myerson, P.N. Patel, K.M. Rubey, M.E. Zamora, M.H. Zaleski, N. Habibi, L.R. Walsh, Y.-W. Lee, D.C. Luther, L.T. Ferguson, O.A. Marcos-Contreras, P.M. Glassman, L.L. Mazaleuskaya, I. Johnston, E.D. Hood, T. Shuvaeva, J. Wu, H.-Y. Zhang, J. V. Gregory, R.Y. Kiseleva, J. Nong, T. Grosser, C.F. Greineder, S. Mitragotri, G.S. Worthen, V.M. Rotello, J. Lahann, V.R. Muzykantov, J.S. Brenner, Supramolecular arrangement of protein in nanoparticle structures predicts nanoparticle tropism for neutrophils in acute lung inflammation, Nat. Nanotechnol. 17 (2022) 86–97. doi:10.1038/s41565-021-00997-y.

[59] H. Harashima, K. Sakata, K. Funato, H. Kiwada, Enhanced hepatic uptake of liposomes through complement activation depending on the size of liposomes., Pharm. Res. 11 (1994) 402–6. doi:10.1023/a:1018965121222.

[60] J. Szebeni, D. Simberg, Á. González-Fernández, Y. Barenholz, M.A. Dobrovolskaia, Roadmap and strategy for overcoming infusion reactions to nanomedicines, Nat. Nanotechnol. 13 (2018) 1100–1108. doi:10.1038/s41565-018-0273-1.

[61] G.L. Ong, M.J. Mattes, Mouse strains with typical mammalian levels of complement activity, J. Immunol. Methods. 125 (1989) 147–158. doi:10.1016/0022-1759(89)90088-4.

[62] C. Lonez, M.F. Lensink, M. Vandenbranden, J.-M. Ruysschaert, Cationic lipids activate cellular cascades. Which receptors are involved?, Biochim. Biophys. Acta - Gen. Subj. 1790 (2009) 425–430. doi:10.1016/j.bbagen.2009.02.015.

[63] C. Lonez, M. Vandenbranden, J.-M. Ruysschaert, Cationic lipids activate intracellular signaling pathways, Adv. Drug Deliv. Rev. 64 (2012) 1749–1758. doi:10.1016/j.addr.2012.05.009.

[64] P.L. Ahl, S.K. Bhatia, P. Meers, P. Roberts, R. Stevens, R. Dause, W.R. Perkins, A.S. Janoff,

Enhancement of the in vivo circulation lifetime of l-α-distearoylphosphatidylcholine liposomes: importance of liposomal aggregation versus complement opsonization, Biochim. Biophys. Acta - Biomembr. 1329 (1997) 370–382. doi:10.1016/S0005-2736(97)00129-6.

[65] E.S. Van Amersfoort, T.J.C. Van Berkel, J. Kuiper, Receptors, Mediators, and Mechanisms Involved in Bacterial Sepsis and Septic Shock, Clin. Microbiol. Rev. 16 (2003) 379–414. doi:10.1128/CMR.16.3.379-414.2003.

[66] H.P. Jersmann, Time to abandon dogma: CD14 is expressed by non-myeloid lineage cells, Immunol. Cell Biol. 83 (2005) 462–467. doi:10.1111/j.1440-1711.2005.01370.x.

[67] D. Christensen, K.S. Korsholm, P. Andersen, E.M. Agger, Cationic liposomes as vaccine adjuvants, Expert Rev. Vaccines. 10 (2011) 513–521. doi:10.1586/erv.11.17.

[68] I. Zanoni, R. Ostuni, L.R. Marek, S. Barresi, R. Barbalat, G.M. Barton, F. Granucci, J.C. Kagan, CD14 Controls the LPS-Induced Endocytosis of Toll-like Receptor 4, Cell. 147 (2011) 868–880. doi:10.1016/j.cell.2011.09.051.

[69] C. Lonez, M. Bessodes, D. Scherman, M. Vandenbranden, V. Escriou, J.-M. Ruysschaert, Cationic lipid nanocarriers activate Toll-like receptor 2 and NLRP3 inflammasome pathways, Nanomedicine Nanotechnology, Biol. Med. 10 (2014) 775–782. doi:10.1016/j.nano.2013.12.003.

[70] I. Zanoni, Y. Tan, M. Di Gioia, J.R. Springstead, J.C. Kagan, By Capturing Inflammatory Lipids Released from Dying Cells, the Receptor CD14 Induces Inflammasome-Dependent Phagocyte Hyperactivation, Immunity. 47 (2017) 697-709.e3. doi:10.1016/j.immuni.2017.09.010.

[71] B. Yu, E. Hailman, S.D. Wright, Lipopolysaccharide binding protein and soluble CD14 catalyze exchange of phospholipids., J. Clin. Invest. 99 (1997) 315–324. doi:10.1172/JCI119160.

[72] K.L. Hawley, C.M. Olson, J.M. Iglesias-Pedraz, N. Navasa, J.L. Cervantes, M.J. Caimano, H. Izadi, R.R. Ingalls, U. Pal, J.C. Salazar, J.D. Radolf, J. Anguita, CD14 cooperates with complement receptor 3 to mediate MyD88-independent phagocytosis of Borrelia burgdorferi, Proc. Natl. Acad. Sci. 109 (2012) 1228–1232. doi:10.1073/pnas.1112078109.

[73] U. Grunwald, X. Fan, R.S. Jack, G. Workalemahu, A. Kallies, F. Stelter, C. Schütt, Monocytes can phagocytose Gram-negative bacteria by a CD14-dependent mechanism., J. Immunol. (1996).

[74] A. Devitt, O.D. Moffatt, C. Raykundalia, J.D. Capra, D.L. Simmons, C.D. Gregory, Human CD14 mediates recognition and phagocytosis of apoptotic cells, Nature. 392 (1998) 505–509. doi:10.1038/33169.

[75] J.-K. Ryu, S.J. Kim, S.-H. Rah, J.I. Kang, H.E. Jung, D. Lee, H.K. Lee, J.-O. Lee, B.S. Park, T.-Y. Yoon, H.M. Kim, Reconstruction of LPS Transfer Cascade Reveals Structural Determinants within LBP, CD14, and TLR4-MD2 for Efficient LPS Recognition and Transfer,

Immunity. 46 (2017) 38–50. doi:10.1016/j.immuni.2016.11.007.

[76] H. Tsukamoto, S. Takeuchi, K. Kubota, Y. Kobayashi, S. Kozakai, I. Ukai, A. Shichiku, M. Okubo, M. Numasaki, Y. Kanemitsu, Y. Matsumoto, T. Nochi, K. Watanabe, H. Aso, Y. Tomioka, Lipopolysaccharide (LPS)-binding protein stimulates CD14-dependent Toll-like receptor 4 internalization and LPS-induced TBK1–IKKϵ–IRF3 axis activation, J. Biol. Chem. 293 (2018) 10186–10201. doi:10.1074/jbc.M117.796631.

Fig. 1. Liposomes functionalized with the TriArg lipopeptide

Liposome formulations used in the study. (a) The structure of the TriArg compound (Cholesterol-GWRRR). (b) TriArg liposomes were formulated both with and without DOPE-PEG_{2000}. (c) Cryogenic transmission electron microscopy (cryoTEM) image of PEGylated liposomes with 6% TriArg lipopeptide.

Fig. 2. Uptake of TopFluor-labeled TriArg liposomes by monocytes, granulocytes, and lymphocytes.

(a) Percentage of TopFluor-positive cells. (b) TopFluor median fluorescence intensity (MFI) of cells. At low percentages of TriArg in the formulation, the liposome uptake is highest in monocytes compared to the granulocytes and lymphocytes. The monocytes uptake further increases as TriArg content increases. At the highest percentages of TriArg tested, there is also increased uptake in granulocytes and slightly in lymphocytes. The trend is the same for PEGylated and non-PEGylated liposomes, but a higher TriArg content is required in the PEGylated liposomes to achieve the same level of cellular uptake. Error bars show SEM, and n=4 except for 3% TriArg (n=8) and 2% TriArg-PEG (n=3). A statistical analysis was carried out, and the resulting p-values for all relevant comparisons are shown in Supplementary Table S1. For gating strategy, see Supplementary Fig. S5.

Fig. 3. Monocyte targeting specificity of TriArg liposomes.

(a) Targeting specificity of all formulations calculated by dividing the MFI of the monocyte population with the MFI of all other cells. (b) Targeting specificity as a function of zeta

potential. (c) Targeting specificity as a function of the charge per 100 lipids. There is no straightforward correlation between the targeting specificity and zeta potential or the charge per 100 lipids in the formulation. The net number of charges per 100 lipids is calculated using that TriArg carries three positive charges and that DOPE-PEG carries one negative charge. Vertical error bars show SEM, and n=4 except for 3% TriArg (n=8) and 2% TriArg-PEG (n=3). Horistontal error bars show SD according to Table 1, n=2-7.

Fig. 4. Monocyte targeting of TriArg liposomes in vivo

(a) Percentage of liposome-positive cells in murine blood 10 min or 4 h after intravenous injection. (b) MFI of cell populations in murine blood 10 min or 4 h after intraveneous injection. There was a higher uptake of the liposomes in the monocytes than in the other cell populations. Inclusion of the TriArg in the liposomes further increased their uptake in monocytes. (c) Blood concentration of Gd-loaded liposomes in mice following intravenous injections. (d) Organ distribution of Gd-loaded liposomes 4 h after intraveneous injection. Incorporation of TriArg in the liposomes decreased the circulation time. More of the PEGylated than the non-PEGylated TriArg liposomes remained in circulation. Error bars show SEM. n = 3-8 for flow cytometry samples, n=5 for organ samples, n = 3 for blood samples. A statistical analysis was carried out, and the resulting p-values for all relevant comparisons are shown in Supplementary Table S2 and S3.

Fig. 5. Complement activation increase in plasma upon exposure to TriArg liposomes

Concentration of complement fragment in plasma normalized to the control sample for every single donor, giving the fold increase in concentration of each complement fragment upon exposure of plasma to liposomes. Concentrations of complement fragments C3a and iC3b increase over the background when exposed to 2% TriArg and 4% TriArg-PEG liposomes, indicating that the complement system is activated. Comparing the increase in Bb (alternative pathway) and C4d fragments (classical or lectin pathway) indicates that the activation is through the alternative pathway. An increase in sC5b9 show that the terminal pathways of complement is also initiated. The 6% TriArg-PEG liposomes do not give rise to a significant increase in concentration for any of the complement fragments tested. n=4, error bars show

SEM. A statistical analysis was carried out, and the resulting p-values for all relevant comparisons are shown in Supplementary Table S4.

Fig. 6. Uptake of TriArg liposomes in leukocytes upon inhibition of the complement system

The complement system in fresh whole human blood was inhibited using the compstatin-analog 4W9A before adding liposomes and investigating leukocyte uptake by flow cytometry. Uptake of liposomes in granulocytes (a) and monocytes (b) upon pre-incubation of blood with either complement inhibitor 4W9A or an inactive linear control peptide. The 4W9A peptide reduces the liposome uptake in the granulocytes, but not in the monocytes or lymphocytes. n=4, error bars show SEM. A statistical analysis was carried out, and the resulting p-values for all relevant comparisons are shown in Supplementary Table S5.

Fig. 7. Inhibition of cellular uptake of TriArg liposomes with a CD14 blocking antibody.

Uptake of liposomes in granulocytes (a) and monocytes (b) upon pre-incubation of blood with either CD14-blocking antibody (clone 18D11) or an isotype antibody (clone MOPC21), as well as in the absence of any antibodies. n=4 except for 2% TriArg and 6% TriArg-PEG with n=6. Error bars show SEM. A statistical analysis was carried out, and the resulting p-values for all relevant comparisons are shown in Supplementary Table S6.

Fig. 8. Proposed pathway for uptake of TriArg liposomes through the CD14 receptor.
CD14 exists both as a membrane bound version (mCD14) and as a soluble version (sCD14). The former is primarily expressed on monocytes, and can thus directly facilitate uptake in monocytes (1). TLR4 signaling, e.g. in response to LPS on gram-negative bacteria, usually happens with the receptor being located at the plasma membrane [63,66]. The TLR4 receptor alone is not able to bind LPS directly, but needs an accessory protein [66]. When this accessory protein is CD14, TLR4 in complex with the ligand is endocytosed, instead of being located at the membrane [66,67]. The CD14/TLR-4 complex can in this way facilitate internalization of the bacteria [71], apoptotic cells [72], or other lipid particles recognized by CD14, e.g. the cationic liposomes presented here. CD14 can directly bind LPS on gram-negative bacteria, PS on apoptotic cells, and a range of other lipids, but the LPS Binding Protein (LBP) can promote this binding (2) [69,73,74], thereby enhancing the TLR4 activation in response to LPS 100-1000 fold compared to serum without LBP. In addition, LBP is involved in CD14-mediated phagocytosis [71]. Furthermore, the soluble version of CD14, sCD14, can facilitate uptake in both monocytes (3) and non-myeloid cells such as granulocytes (4). The figure illustrates how CD14 could thus serve as a co-receptor driving endocytosis of cationic liposomes in both CD14 positive monocytes and in cells with low or none mCD14 expression. It should be noted, that a low degree of mCD14 expression in granulocytes could also mediate uptake in these cells in parallel to the complement-mediated opsonization. The results presented in this paper supports that this LBP/CD14-pathway, previously demonstrated for monocyte phagocytosis of bacteria [71], is also involved in uptake of cationic liposomes. In parallel, however, the complement system can also facilitate uptake in granulocytes (5). This pathway seems to dominate when the TriArg content is increased (see data in Fig. 7).

Table 1. Characteristics of TriArg liposomes included in the study

Overview of the liposome formulations tested in the present study. The 30 mol% cholesterol in the formulations does not include the 1-8% cholesterol on the TriArg lipopeptide. The results are shown as the mean ± SD for all batches produced of a given formulation. Between two and seven batches were produced of each formulation.

Declaration of interests

☐ The authors declare that they have no known competing financial interests or personal relationships that could have appeared to influence the work reported in this paper.

☒The authors declare the following financial interests/personal relationships which may be considered as potential competing interests:

T.L. Andresen, L. Parhamifar and R. Münter have IP on cationic liposomes for immunotherapy (Patent number WO2019012107). The authors declare no other relevant affiliations with financial interests.

Statement of Significance

for manuscript

Mechanisms of Selective Monocyte Targeting by Liposomes Functionalized with a Cationic, Arginine-Rich Lipopeptide

Monocytes are attractive targets for immunotherapies of cancers, infections and autoimmune diseases. Specific delivery of immunostimulatory drugs to monocytes is typically achieved using ligand-targeted drug delivery systems, but a simpler approach is to target monocytes using cationic liposomes. To achieve this, however, a deep understanding of the mechanisms governing the interactions of cationic liposomes with monocytes and other leukocytes is required. We here investigate these interactions using liposomes incorporating a cationic arginine-rich lipopeptide. We demonstrate that monocyte targeting can be achieved by fine-tuning the lipopeptide content in the liposomes. Additionally, we reveal that the CD14 receptor is involved in the targeting process, whereas the complement system is not. These mechanistic findings are critical for future design of monocyte-targeting liposomal therapies.